A Novel Slurry-Based Biomass Reforming Process

Final Report

Project Period:	2 May 2005 to 30 June 2011
Date of Report:	30 September 2011
Award Number:	DE-FG36-05GO15042
Principle Investigator	Sean C. Emerson
Authors:	Sean C. Emerson, Timothy D. Davis, A. Peles, Ying She, Joshua Sheffel, Rhonda R. Willigan, Thomas H. Vanderspurt, & Tianli Zhu
Submitting Organization:	United Technologies Research Center 411 Silver Lane East Hartford, CT 06108
Team Members:	Energy & Environmental Research Center University of North Dakota, Grand Forks, ND

This research used resources of the National Center for Computational Sciences at Oak Ridge National Laboratory, which is supported by the Office of Science of the Department of Energy under Contract DE-AC05-00OR22725.

Work performed under the DOE Grant DE-FG36-05GO15042 was authorized in part under a research license for the Aqueous Phase Reforming Process (Patent 6,699,457; 6,694,757; 6,694,758 [and all other licensed issued patents]) from Virent Energy Systems in Madison, Wisconsin.

Contents

List of Figures

List of Tables

1 Executive Summary

This project was focused on developing a catalytic means of producing H_2 from raw, ground biomass, such as fast growing poplar trees, willow trees, or switch grass. The use of a renewable, biomass feedstock with minimal processing can enable a carbon neutral means of producing H_2 in that the carbon dioxide produced from the process can be used in the environment to produce additional biomass. For economically viable production of H_2, the biomass is hydrolyzed and then reformed without any additional purification steps. Any unreacted biomass and other byproduct streams are burned to provide process energy. Thus, the development of a catalyst that can operate in the demanding corrosive environment and presence of potential poisons is vital to this approach.

The concept for this project is shown in Figure 1. The initial feed is assumed to be a >5 wt% slurry of ground wood in dilute base, such as potassium carbonate (K_2CO_3). Base hydrolysis and reforming of the wood is carried out at high but sub-critical pressures and temperatures in the presence of a solid catalyst. A Pd alloy membrane allows the continuous removal of pure H_2, while the retentate, including methane is used as fuel in the plant.

The project showed that it is possible to economically produce H_2 from woody biomass in a carbon neutral manner. Technoeconomic analyses using HYSYS and the DOE's H2A tool [1] were used to design a 2000 ton day^{-1} (dry basis) biomass to hydrogen plant with an efficiency of 46% to 56%, depending on the mode of operation and economic assumptions, exceeding the DOE 2012 target of 43%. The cost of producing the hydrogen from such a plant would be in the range of \$1/kg H_2 to \$2/kg H_2. By using raw biomass as a feedstock, the cost of producing hydrogen at large biomass consumption rates is more cost effective than steam reforming of hydrocarbons or biomass gasification and can achieve the overall cost goals of the DOE Fuel Cell Technologies Program.

The complete conversion of wood to hydrogen, methane, and carbon dioxide was repeatedly demonstrated in batch reactors varying in size from 50 mL to 7.6 L. The different wood sources (e.g., swamp maple, poplar, and commercial wood flour) were converted in the presence of a heterogeneous catalyst and base at relatively low temperatures (e.g., 310 °C) at sub-critical pressures sufficient to maintain the liquid phase.

Both precious metal and base metal catalysts were found to be active for the liquid phase hydrolysis and reforming of wood. Pt-based catalysts, particularly Pt-Re, were shown to be more selective toward breaking C-C bonds, resulting in a higher selectivity to hydrogen versus methane. Ni-based catalysts were found to prefer breaking C-O bonds, favoring the production of methane. The project showed that increasing the concentration of base (base to wood ratio) in the presence of Raney Ni catalysts resulted in greater selectivity toward hydrogen but at the expense of increasing the production of undesirable organic acids from the wood, lowering the amount of wood converted to gas. It was shown that by modifying Ni-based catalysts with dopants, it was possible to reduce the base concentration while maintaining the selectivity toward hydrogen and increasing wood conversion to gas versus organic acids.

The final stage of the project was the construction and testing of a demonstration unit for H_2 production. This continuous flow demonstration unit consisted of wood slurry and potassium carbonate feed pump systems, two reactors for hydrolysis and reforming, and a gas-liquid separation system. The technical challenges associated with unreacted wood fines and Raney Ni catalyst retention limited the demonstration unit to using a fixed bed Raney Ni catalyst form. The lower activity of the larger particle Raney Ni in turn limited

the residence time and thus the wood mass flow feed rate to 50 g min^{-1} for a 1 wt% wood slurry. The project demonstrated continuous H_2 yields with unmodified, fixed bed Raney Ni, from 63% to 100% with corresponding H_2 selectivities of 6% to 21%, for periods of several hours. The fixed bed form of the Raney Ni exhibited signs of deactivation which requires further study.

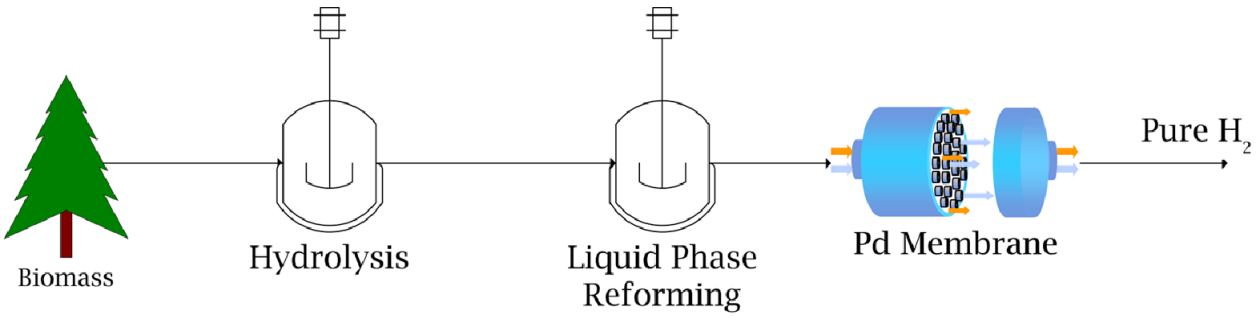

Figure 1: The UTRC approach to biomass slurry reforming.

1.1 Understanding of the Area Investigated

The most important contribution to the technical community from this project has been demonstrating that different wood feedstocks can be completely converted to gas (hydrogen, methane, and carbon dioxide) and the modeling and analysis with simple model compounds to elucidate the chemical pathway. From the beginning of this project, the focus was on a process that would use raw, untreated biomass as a feedstock. Although other organizations have conducted work on liquid or aqueous phase reforming of biologically derived feedstocks, until recently the research and development has been focused on simpler compounds such as sorbitol or glycerol. These compounds have an advantage in that they are easier to work with in a laboratory environment, but have the disadvantage of being more expensive than the biomass from which they are derived. By showing that raw woody biomass can be gasified in a low temperature process, the project has revealed a viable technical path to low cost hydrogen production.

1.2 Technical Effectiveness & Economic Feasibility

As described in Section 2.1, extensive technoeconomic modeling occurred throughout the course of this project. By using raw biomass as a feedstock, the cost of producing hydrogen at large biomass consumption rates (e.g., 2000 ton day^{-1}) is less expensive than the DOE technical targets set for biomass gasification and can achieve the overall cost goals of the DOE Fuel Cell Technologies Program. The technology has been repeatedly and successfully demonstrated at a laboratory scale in batch reactors and with some limited success in a continuous production mode largely attributable to the small scale of the system. To make this process a commercial reality will require further technology development focused on continuous hydrogen production, including a demonstration at a larger than laboratory scale.

1.3 Benefit to the Public

Subject to the constraints of biomass availability, the UTRC Biomass to H_2 process has the potential to benefit the public by offering an economically viable, renewable, and carbon

neutral means of producing hydrogen using domestic resources to displace foreign imports of energy. The U.S. Department of Energy began the Hydrogen Fuel Initiative in 2003 with the objective of commercializing hydrogen fuel cell vehicles by 2020. The motivation for producing hydrogen on a large scale is that it can "reduce our dependence on imported oil and benefit the environment by reducing greenhouse gas emissions and criteria pollutant emissions that affect our air quality."[2]

As part of the DOE Fuel Cell Technology Program, the Hydrogen Production Technical Team (HPTT) of the FreedomCAR and Fuel Partnership, created a roadmap to "identify the key challenges and priority research and development (R&D) needs associated with various hydrogen fuel production technologies."[3] The roadmap characterized various technologies into near-term, mid-term, and long-term development pathways. This project is considered under the DOE Fuel Cell Technology Program to be a form of Biomass Gasification, which the HPTT has identified as a mid-term technical solution to widespread production of hydrogen. Thus, the liquid phase reforming pathway described in this report has been shown to be an economically viable approach to produce hydrogen from biomass and offers the next step in the widespread use of hydrogen.

1.4 Accomplishments

There were four key objectives for this project:

- Develop an initial reactor and system design, with cost projections, for a biomass slurry hydrolysis and reforming process for hydrogen (H_2) production from woody biomass
- Develop a cost effective catalyst for liquid phase reforming of biomass
- Perform a proof-of-concept demonstration of a micro-scale pilot system based on liquid-phase reforming of biomass
- Demonstrate that the proposed H_2 production system will meet the 2012 efficiency and cost targets of 43% LHV and \$1.60/kg H_2 for a 2000 ton day^{-1} (dry wood) plant

All of the objectives were met during the course of the project. Section 2.1 details the technoeconomic analysis around the first and last objectives, where cost and efficiency projections were made for a 2000 ton day^{-1} (dry basis) wood plant. The tables in that Section compare the plant design to the DOE 2012 targets of hydrogen cost, total capital investment, and energy efficiency. In all cases, the DOE hydrogen cost and energy efficiency targets can be met by the biomass to H_2 process developed in this project. Overall capital investment remained a challenge, depending on the assumptions for plant operation, including assumptions about hydrogen separation technology and the hydrogen delivery pressure.

The second project objective for the development of cost effective catalysts was achieved through the use of nickel-based catalysts. Although precious metal catalysts, such as Pt-Re, were found to have high activity and selectivity toward hydrogen production, it was shown that Ni catalysts could perform the same function, provided they were modified with dopants to enhance their selectivity toward hydrogen. Most of this work was performed using very high surface area Raney Ni powder. However, a fixed bed form of the Raney Ni, which was used in a demonstration system, exhibited signs of deactivation which requires further study.

The third project objective, a proof-of-concept demonstration of a micro-scale pilot system was achieved. A demonstration unit for H_2 production was constructed that consisted of wood slurry and potassium carbonate feed pump systems, two reactors for hydrolysis and reforming, and a gas-liquid separation system. The technical challenges

associated with unreacted wood fines and Raney Ni catalyst retention at small scale limited the unit to using the low surface area, fixed bed Raney Ni catalyst form. The lower activity of the larger particle Raney Ni in turn limited the residence time and thus the wood mass flow feed rate to 50 g min^{-1} for a 1 wt% wood slurry. However, the project demonstrated continuous flow H_2 yields with unmodified, fixed bed Raney Ni, from 63% to 100% with corresponding H_2 selectivities of 6% to 21%, for periods up to 4 hours.

2 Results

2.1 System Modeling, Energy, & Economic Analysis

2.1.1 Original 2000 ton day^{-1} Design with Acid Hydrolysis

The original basic concept for this project is shown in Figure 2. The initial feed was assumed to be a 10 wt% slurry of ground poplar wood in dilute acid. The acid would hydrolyze the cellulose and hemicellulose in the wood to produce a reformable mixture for the catalyst to be developed during this project. To avoid char formation and to reach hydrogen production goals, an optional hydrogenation step was considered in conjunction with the hydrolysis step. The reformable mixture would be reacted in the liquid phase over a mixed metal Pt based rafts (Pt-MM)/ mixed metal oxide catalyst to convert the hydrolyzed biomass to hydrogen. A palladium alloy membrane would be used to remove the pure hydrogen thus limiting methane formation, while the retentate was used as fuel in the proposed plant.

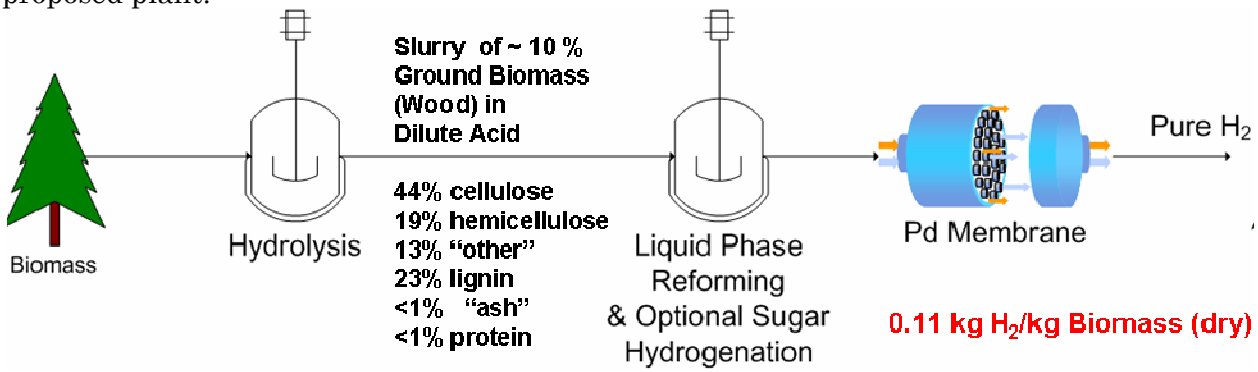

Figure 2: The UTRC approach to biomass slurry reforming from the beginning of the project in 2005.

During the initial project work in 2005 and 2007, a system plant design layout, with biomass as a feed to be hydrolyzed to reformable oxygenates and consequently reformed to H_2 and CO_2, was developed. For the purposes of this plant design, glucose was chosen as a surrogate oxygenate. Using the HYSYS process simulator package, the process, shown in Figure 3, was modeled and simulated.

In this plant design, 2000 ton day^{-1} of dry biomass was fed to produce hydrogen. Several key features were implemented in the design in order to achieve high system efficiency and minimize air pollution. First, unconverted lignin in the effluent from the reformer, along with unrecovered H_2 and fuel gases, was sent to the burner for combustion to recover energy. Second, the burner exhaust gas and other hot process streams were passed through heat exchangers to use process heat effectively. Third, the system was further process

intensified by recycling much of the hot water used for hydrolysis. Finally, the system included an SO_2 oxidizer and an SO_3 scrubber to remove sulfur from the plant exhaust and also to recover sulfuric acid, minimizing emission of sulfur compounds.

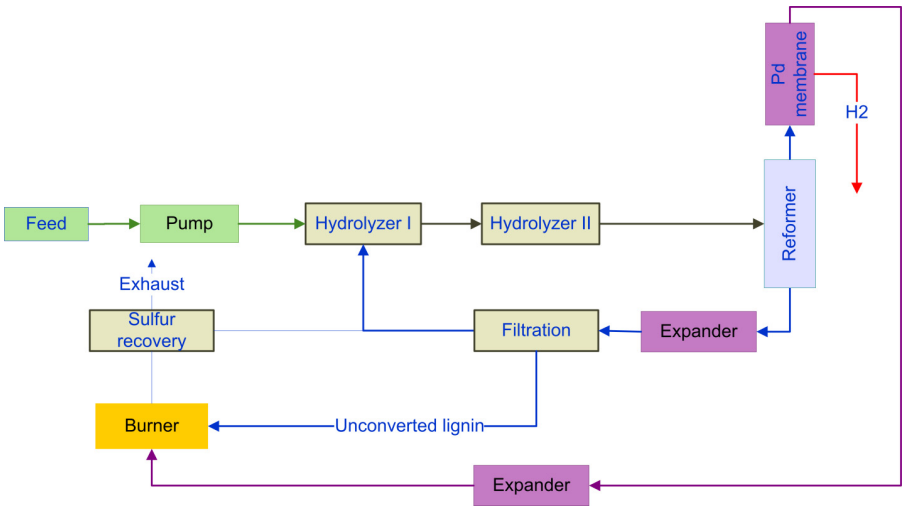

Figure 3: Simplified block diagram of a biomass to hydrogen plant using acid hydrolysis.

There are several ways of calculating the efficiency of a hydrogen production plant. In 2005, when much of the plant design model was constructed, UTRC originally used a definition, which will be described here as the LHV (lower heating value) energy efficiency, shown in Equation (1). The DOE's H2A economic analysis tool [1, 4] subsequently introduced two additional efficiency definitions, the process energy efficiency and the plant H_2 efficiency, shown in Equations (2) & (3), respectively. The plant H_2 efficiency was used for all work from 2007.

$$\text{LHV energy efficiency} = \frac{\text{LHV of product } H_2 + \text{Energy recovered} - \text{Energy consumed}}{\text{LHV of biomass feed}} \quad (1)$$

$$\text{Process energy efficiency} = \frac{\text{LHV of product } H_2 + \text{Energy recovered}}{\text{LHV of biomass feed} + \text{Energy consumed}} \quad (2)$$

$$\text{Plant } H_2 \text{ efficiency} = \frac{\text{LHV of product } H_2}{\text{LHV of biomass feed} + \text{Energy consumed}} \quad (3)$$

A statistically designed system model parameter study was conducted by UTRC that revealed the nine variables that had the strongest effect on system efficiency [5]. This study lead to the development of an empirical function that described the effect of the most important operating parameters on the system efficiency, taking into account any interactions between the parameters that occur. The parameter study revealed two key features of a biomass to hydrogen plant based on liquid phase reforming**. The first was that the reforming conversion of sugars such as glucose can be as low as 75% and still achieve the DOE's 2012 efficiency targets. The second was that the production of alkanes, such as methane, was not detrimental to system efficiency, as the alkanes can be burned to produce energy to operate the plant.**

The acid-based hydrolysis baseline 2000 ton day^{-1} biomass to hydrogen plant model was designed using the process simulator HYSYS and resulted in a plant hydrogen efficiency of **46.6%**. The economic analysis of the baseline plant design using the H2A tool (version 1.0 [4]) showed that a hydrogen production cost of **$1.58/kg H_2** was attainable.

2.1.2 Design Switch to 2000 ton day^{-1} with Base Hydrolysis

Based on the results from the batch reactor experiments with acid and base addition described later in this report, the design basis for the plant was changed from acid hydrolysis to base hydrolysis. The results with base hydrolysis showed that essentially all of the biomass (wood) can be converted into gas products. The overall concept was adjusted so that the initial feed was assumed to be a >5 wt% slurry of ground poplar wood in dilute base. Potassium carbonate, derived from wood ash, is considered an effective base. Base hydrolysis of the wood in the adjusted concept is carried out at high but sub-critical pressures and temperatures in the presence of a high surface area, high metal dispersion, large pore, base stable Pt-Re/$Ce_{(1-x)}Zr_xO_2$ catalyst. A palladium alloy membrane allows the continuous removal of pure hydrogen, thus limiting methane formation, while the retentate is used as fuel in the plant.

In 2009, the baseline techno-economic analysis was updated to reflect the use of base instead of acid for the hydrolysis process. A simplified process block diagram is shown in Figure 4. The model feedstock representing the wood was adjusted to be 72.6% cellulose, 27% lignin surrogate ($C_8H_8O_3$) and 0.4% ash. The hydrolysis was reduced to a single step process where the alkali is derived from potassium in the wood and where the lignin is completely hydrolyzed. The sulfur removal process was eliminated from the system. The burner system was also adjusted to reflect the combustion of process derived gases, such as methane, rather than unconverted lignin as the experimental work had shown that essentially 100% of the wood can be converted into gas products. The reformer size was also reduced based on the kinetic results from flow reactor experiments described later in this report. The updated baseline 2000 ton day^{-1} biomass to hydrogen plant designed using the process simulator HYSYS showed a plant hydrogen efficiency of **53.9%**. The preliminary economic analysis of the baseline alkaline plant design also showed that a hydrogen production cost of **$1.27/kg H_2** could be attainable with a total capital investment of **$203M**.

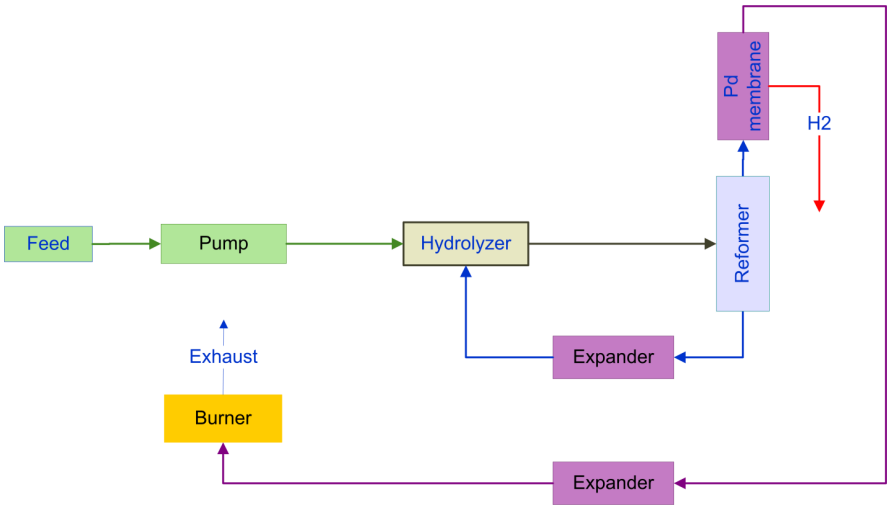

Figure 4: Simplified block diagram of a biomass to hydrogen plant using alkaline hydrolysis.

2.1.3 Impact of Increased H_2 Delivery Pressure on Alkali-Based Plant

In 2010, the baseline model was updated again to reflect the use of base metal catalysts instead of precious metal catalysts as well as to increase the delivery pressure of the hydrogen from the plant. The economics of the alkali hydrolysis based plant design using Ni-based catalysts were updated using the new version of the H2A tool from the DOE [1]. For all cases, a Pd membrane based separator was used to produce >99.9999% H_2 from the process for fuel cell use. For the baseline economics, the H_2 was then compressed from atmospheric pressure up to a pipeline delivery pressure of 300 psia. The use of a H_2 compression system was a more economical investment compared to using a larger Pd membrane separator operating with a 300 psia back pressure. However, the electrical demands of the plant increase significantly due to the compression system.

For all economic scenarios reported here, there are several assumptions common to the HYSYS/H2A model analyses. The wood feedstock price was set at $41/ton to keep with the DOE's cost target basis. The cost of K_2CO_3 feed for the plant was set at $900/ton and the design assumes that 95% of the K_2CO_3 will be recycled within the system. The reforming catalyst was assumed to be equivalent to Raney Ni at a cost of $20/lb with catalyst replacement occurring every 3 years. The reformer liquid residence time was fixed at 16 minutes with a catalyst to wood mass ratio set at a very conservative 20.

Three different Pd membrane scenarios were used to evaluate variability in the plant economics, as the membrane is a dominant factor in the capital cost of the plant design. One scenario assumes a very modest H_2 flux of 60 $ft^3ft^{-2}h^{-1}$ and a membrane cost of $1500/$ft^2$, which is achievable by today's technology. The second scenario assumes that the H_2 flux is higher, 200 $ft^3ft^{-2}h^{-1}$, but with the same membrane cost. The final scenario assumes a high performance membrane with a H_2 flux of 200 $ft^3ft^{-2}h^{-1}$, but with a dramatically lower cost of $100/$ft^2$. The second scenario is used for comparison against the DOE targets (shown in Table 1) with the results of the other two membrane scenarios used to report an upper and lower bound to the costs metrics. The plant hydrogen efficiency was calculated to be **51.1%** for a hydrogen production cost of **$1.54/kg H_2**.

Table 1: HYSYS/H2A analysis results for an alkali hydrolysis based plant design using Ni-based catalysts with a 300 psia H_2 delivery pressure as measured against the DOE's technical targets for biomass gasification/pyrolysis hydrogen production.

Characteristics	Units	2012 Target	Current Status
Hydrogen Cost (Plant Gate)	$/gge	1.60	1.54 (1.31–2.11)
Total Capital Investment	$M	150	170 (117–304)
Energy Efficiency	%	43	51.1

2.1.4 Impact of Mode of Operation on Alkali-based Plant Economics

In general, the hypothetical 2000 ton day^{-1} (dry) biomass plant can be run in three different modes. The first of these modes would use an inexpensive fuel source, such as natural gas, to provide the heat required to operate the endothermic hydrolysis, reforming, and H_2 separation processes. In addition, significant electricity is brought into the plant from an external grid to run the pumps, blower, and compression systems. This "natural gas mode" results in the best cost of H_2 production, but at the expense of carbon neutrality. Table 2 shows the summary of the "natural gas" mode plant design compared to the DOE targets.

Table 2: Technoeconomic modeling results for "natural gas" mode operation compared to the DOE targets.

Characteristics	Units	2012 Target	2000 tpd Plant Design
Hydrogen Cost (Plant Gate)	$/gge	1.60	1.27 (1.05–1.84)
Total Capital Investment	$M	150	188 (116–370)
Energy Efficiency	%	43	56.3

The second mode of operation assumes that the plant is operated to achieve "carbon neutrality" in terms of CO_2 emissions, not counting the secondary emissions that come from electricity provided from the grid for H_2 compression. Instead of using inexpensive fossil fuels to provide the heat required for the plant, more H_2 is allowed in the retentate stream from the membrane separator, and burned to produce heat. This carbon neutrality comes at a cost, both in terms of the H_2 cost and the efficiency, as H_2 that could be delivered from the plant is diverted to heat production instead. Table 3 shows the summary of the "carbon neutral" mode plant design compared to the DOE targets.

Table 3: Technoeconomic modeling results for "carbon neutral" mode operation compared to the DOE targets.

Characteristics	Units	2012 Target	2000 tpd Plant Design
Hydrogen Cost (Plant Gate)	$/gge	1.60	1.54 (1.31–2.11)
Total Capital Investment	$M	150	170 (117–304)
Energy Efficiency	%	43	51.1

The final mode of operation assumes that the plant is operated in a "carbon neutral; electric grid independent" mode. To achieve electric grid independence, the electrical demand from the H_2 compression system was reduced to the point that electricity generated from expanders in the plant could provide all the power needed. As a result, the delivery pressure of the H_2 was also reduced to 44.09 psia. The cost of H_2 in this scenario does not change relative to the "carbon neutral" mode, but the capital costs are lowered and the plant efficiency is reduced. Table 4 shows the summary of the "carbon neutral; electric grid independent" mode plant design compared to the DOE targets.

Table 4: Technoeconomic modeling results for "carbon neutral; electric grid independent" mode operation compared to the DOE targets.

Characteristics	Units	2012 Target	2000 tpd Plant Design
Hydrogen Cost (Plant Gate)	$/gge	1.60	1.54 (1.31–2.11)
Total Capital Investment	$M	150	164 (117–283)
Energy Efficiency	%	43	46.1

2.1.5 Proof-of-Concept Demonstrator Technoeconomic Analysis

To better understand the performance of the UTRC proof-of-concept demonstrator, described in Section 2.6, to produce H_2 from biomass feedstock, a HYSYS system model was established. The model simulated H_2 production from biomass feedstock for the demonstrator to help analyze system efficiency. The HYSYS model consisted primarily of a hydrolyzer and a liquid-phase reformer. The CH_4 exiting the reformer was accounted for along with the H_2 and thermal energy inputs to the system. No H_2 separation membrane was included in this simulation.

A system efficiency of **46%** was calculated from the HYSYS model of the demonstrator assuming the production of 2 kW of H_2 thermal energy (2.5 kW for H_2+CH_4). This was lower than the 51% efficiency calculated for an integrated, standalone, "carbon neutral" plant due to the absence of a recycle stream for water, a Pd membrane, and an integrated burner.

At the end of the experimental program, a technoeconomic analysis was also performed to investigate the impact of scaling up the demonstrator system from Task 3. The main assumptions for this study were: (1) that there was no H_2 purification with a Pd membrane, (2) that the system was operated in a carbon neutral mode (i.e., the product gas was burned to produce the heat required for the hydrolysis and reforming steps), and (3) that the chemistry used in the HYSYS simulations was updated to match the experimental results for the Raney Ni-based catalyst. Figure 5 shows the variation in H_2 production cost and overall plant capital cost as a function of the system scale, which is represented by the biomass feed rate to the plant on a dry basis.

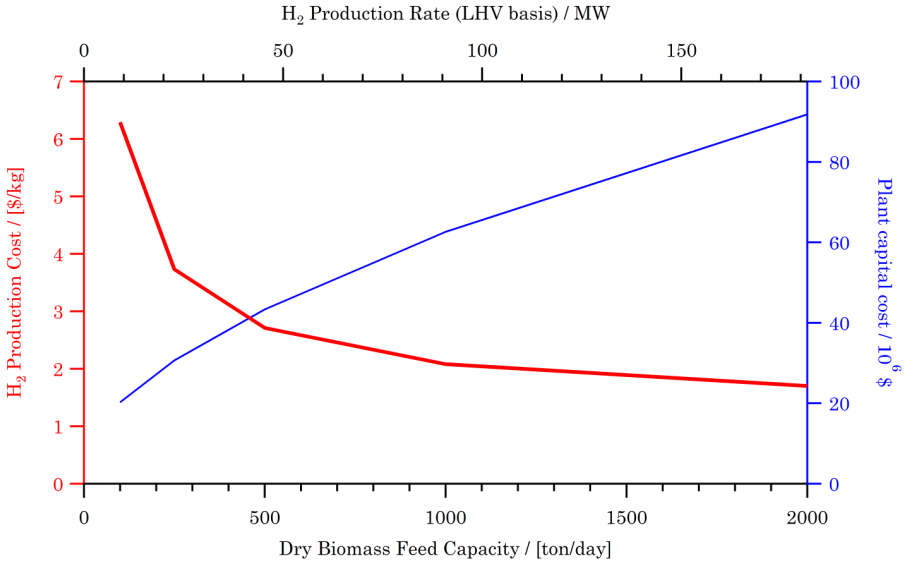

Figure 5: Impact of biomass feed rate on H_2 production cost for a simplified demonstration system from Task 3 operated in a carbon neutral mode without H_2 purification. The system efficiency is 49.3% with a net hydrogen yield of 0.065 kg H_2/kg biomass (dry basis).

The efficiency of this scaled up demonstrator system was calculated to be **49.3%**. However, to maintain carbon neutrality, half of the system's product gas had to be burned to provide heat for the endothermic reactions in the plant. As a result, the overall H_2 yield was reduced to 0.065 kg H_2/kg biomass (dry basis), which was approximately half of the overall H_2 yield in the simulations discussed above of a 2000 ton day^{-1} plant. The overall capital cost for a 2000 ton day^{-1} dry biomass demonstrator was reduced relative to the baseline plant design operated in a carbon neutral mode (**$92M** versus $170M). This lower overall H_2 yield resulted in a H_2 production cost of **$1.70/kg H_2** versus the baseline carbon neutral production cost of $1.54/kg H_2 discussed above.

To remain cost competitive with H_2 production via natural gas steam reforming, the cost of producing H_2 should be less than $3/kg H_2. Using this criterion, the minimum plant scale required to compete directly with hydrocarbon steam reforming is approximately 500 ton day^{-1} biomass (dry). This size plant is equivalent to 45.4 MW of H_2 on a lower heating value basis.

2.2 Liquid Phase Reforming in Batch Reactors

2.2.1 Glycerol Reforming under Acidic Conditions

From 2007 to 2008, the project switched focus from system and economic modeling to catalyst development. The modeling work (see Section 2.1.1) indicated that reforming conversion could be as low as 75% and still achieve the DOE's 2012 efficiency targets. Also, it was found that the production of alkanes, such as methane, was not detrimental to system efficiency because the alkanes can be burned to produce energy to operate the process. Thus, the techno-economic modeling established boundaries for catalyst performance.

As part of the catalyst development effort, significant atomistic and chemical reaction modeling was performed to identify the best candidate oxide supports for platinum. In parallel, experiments were performed in autoclaves to identify conditions (temperature and acid concentration) where model sugars and sugar alcohols would not form significant amounts of char. Based on these char experiments, glycerol was selected as the first model compound to be used for catalyst activity screening.

Many experiments were performed in a semi-batch, high pressure, liquid phase reactor to establish the activity of different catalyst candidates. As part of this catalyst screening activity, a 0.5% Pt/Al_2O_3 benchmark catalyst from Alfa/Aesar was also tested. Lack of reproducibility of the reactor results for the 0.5% Pt/Al_2O_3 catalyst resulted in a root cause investigation of both the catalyst and the reactor setup. It was determined that part of the reproducibility issue was due to the benchmark catalyst itself, which lost platinum to the reaction solution, and was mitigated by recalcining the as received material; and part was due to reactor design issues. The reactor design used a nitrogen sweep gas to remove gas products and impart some mixing, but the low diffusivity of glycerol and small variations in catalyst pellet placement within the reactor contributed to reproducibility issues.

As a result of the root cause investigation, the catalyst screening work was moved to a larger scale, stirred, zirconium autoclave. Proper pretreatment of the 0.5% Pt/Al_2O_3 catalyst, combined with increased agitation from the autoclave impeller, resulted in very reproducible activity measurements. The relative activity of many of the catalysts investigated during this project were comparable to that of the 0.5% Pt/Al_2O_3 catalyst, but the use of a good water gas shift (WGS) catalyst, such as Pt on ceria-zirconia, enabled hydrogen production at temperatures <190 °C while the baseline alumina catalyst had no hydrogen production below 210 °C. Figure 6 shows the main product gas concentrations in the nitrogen sweep gas as the temperature is increased in the autoclave using a vendor scaled-up 2% $Pt/Ce_{0.6}Zr_{0.4}O_2$ WGS catalyst. The selectivity toward hydrogen production from glycerol was 93% throughout the temperature range.

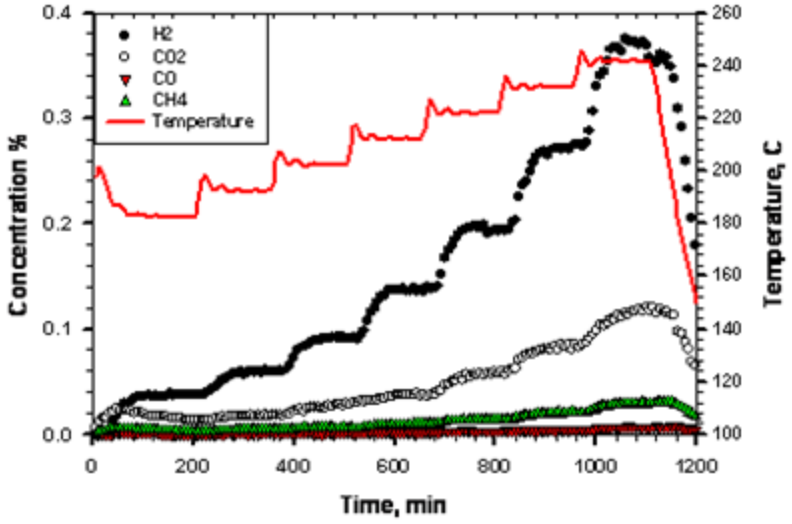

Figure 6: Gas concentrations in nitrogen sweep gas as a function of increasing temperature and reaction time produced from liquid phase reforming of 2.5 wt% glycerol (0.283 mol L^{-1}) in the presence of a vendor scaled-up 2% $Pt/Ce_{0.6}Zr_{0.4}O_2$ WGS catalyst.

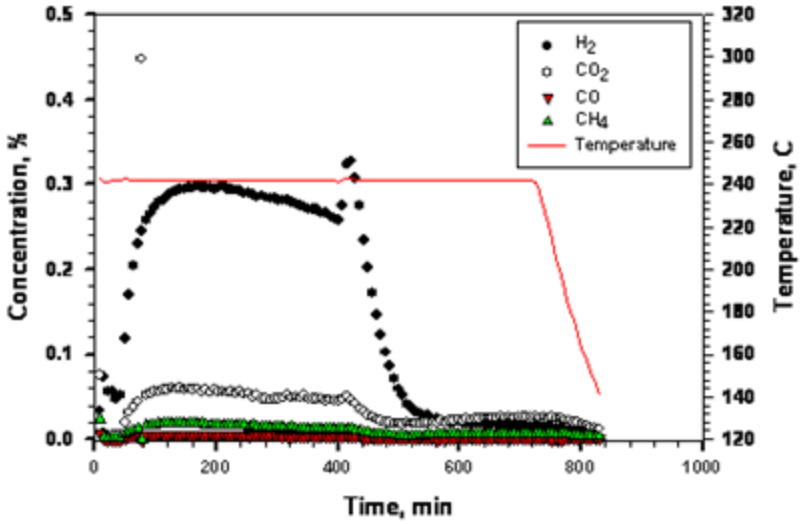

Figure 7: Gas concentrations in nitrogen sweep gas for an autoclave test at 240 °C with a 0.5% Pt/Al_2O_3 catalyst in a 2.5 wt% glycerol solution (0.283 mol L^{-1}). After 400 minutes of operation, 0.1 mol L^{-1} of $KHSO_4$ was injected into the autoclave resulting in a rapid deactivation of the hydrogen production.

In the initial reactor design, the presence of sulfur and acid in the form of $KHSO_4$ had a small effect on catalyst performance. However, with the larger autoclave and increased agitation, addition of $KHSO_4$ terminated hydrogen production and increased the production of higher hydrocarbons such as ethane. Figure 7 shows typical gas concentration results in the nitrogen sweep gas for an autoclave run at 240 °C with the 0.5% Pt/Al_2O_3 catalyst in a 2.5 wt% glycerol solution (0.283 mol L^{-1}). After 400 minutes of operation, 0.1 mol L^{-1} of

$KHSO_4$ was injected into the autoclave resulting in a rapid decrease in the hydrogen production.

In 2008, the use of base instead of acid for hydrolysis was investigated. The use of a base, such as K_2CO_3, resulted in an increase in hydrogen production rates for the baseline 0.5% Pt/Al_2O_3 catalyst by a factor of three while also minimizing char formation from the glycerol. In addition to the first base experiments, some initial experiments were performed on wood chips in the presence of a catalyst and base resulting in the first direct production from wood in the aqueous phase.

2.2.2 Hydrogen Production from Swamp Maple under Basic Conditions with Precious Metal Catalysts

Hydrogen was produced by the alkaline phase reforming of swamp maple (*Acer rubrum*) saw dust. However alkaline hydrolysis caused a foaming problem in UTRC's autoclave reactor system. This foaming resulted in a system redesign. The large zirconium autoclave was replaced by a smaller, 50 mL titanium reactor designed to minimize the transport of foam out of the reactor. The glycerol reforming results with this new reactor were reproducible. Based on the understanding obtained from the 50 mL titanium reactor, the autoclave reactor system was also redesigned to handle foaming issues.

Because acidic media was shown to shut down oxygenate reforming reactions over Pt catalysts, a study of biomass reforming in alkali hydrolysis media in a zirconium autoclave reactor was undertaken. **The two major learnings from this study were: (1) that the production of hydrogen from swamp maple requires base and (2) that the hydrogen production decreases as the concentration of base increases.** Standard test conditions in the zirconium autoclave were 240 °C, 1640 psi with a nitrogen sweep gas rate of 0.5 L min^{-1} (STP) and 10 wt% swamp maple (80 g on an as received basis or 49.8 g on a vacuum oven dried basis). Figure 8 shows the hydrogen production with 0.6M KOH solution over a 2 wt% $Pt/Ce_{0.6}Zr_{0.4}O_2$ catalyst.

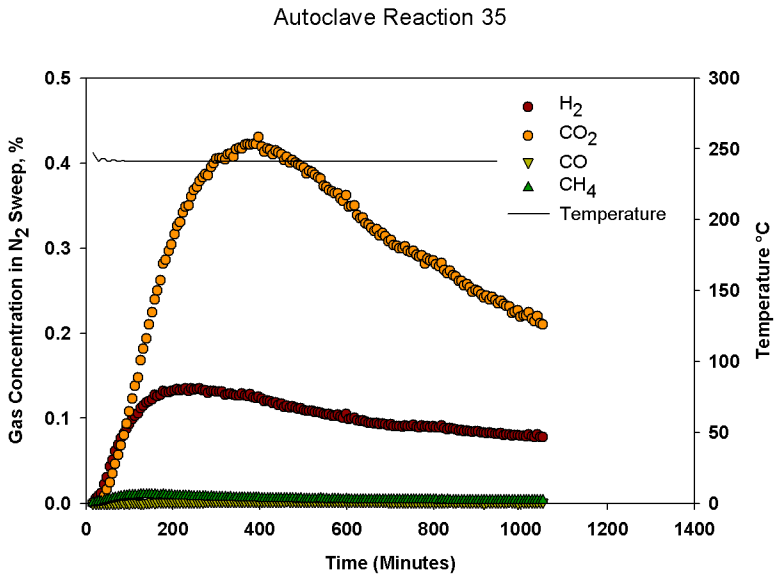

Figure 8: Effluent gas concentration for aqueous phase reforming of 10 wt% swamp maple in 0.6 M KOH solution at 240 °C with 1 g of a 2 wt% $Pt/Ce_{0.6}Zr_{0.4}O_2$ catalyst.

One issue encountered during the initial work was the relatively quick deactivation of the reforming reactions. To determine whether this was a shutdown of hydrolysis pathways, a series of experiments was run to study the effect of the addition of a second aliquot of alkali solution. Data for the reaction run at 240 °C with a 0.2 M KOH solution are given in Figure 9. It was discovered that the addition of a second aliquot of KOH caused a drastic decrease in gas production, ultimately shutting down production. In addition, during all of these experiments, it was found that hydrolysis in alkali solutions produced a significant amount of foaming that was detrimental to the experimental setup. Further analysis to determine the source of the foam was required.

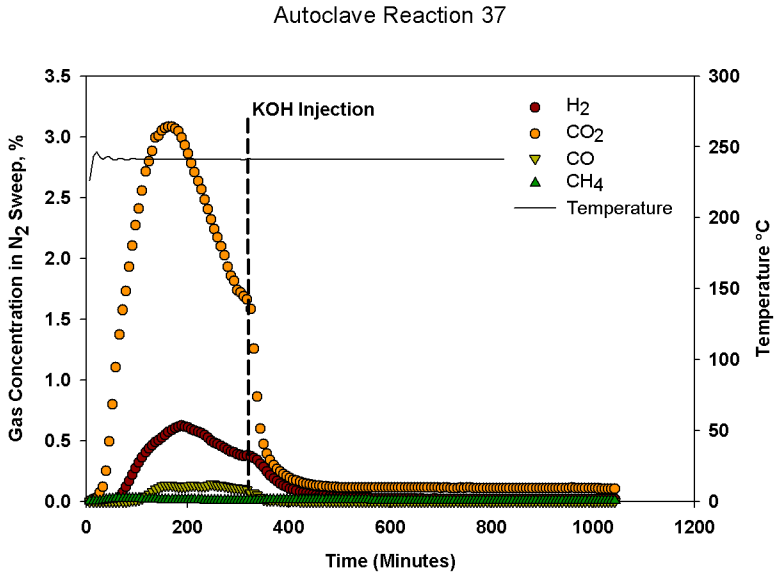

Figure 9: Effluent gas concentration for the aqueous phase reforming of 10 wt% swamp maple in 0.2 M KOH solution at 240 °C with 1 g of 2 wt% Pt/$Ce_{0.6}Zr_{0.4}O_2$ catalyst followed by additional KOH injection.

2.2.3 Reforming of Model Compounds to Investigate Swamp Maple Results

To better understand the chemistry involved in the system, simple model compounds in acid and alkali environments were studied. Glycerol, ethylene glycol, and methanol were chosen as model compounds, offering the ability to study the effect of the number of C-C bonds in the reaction. The goals of this brief study were as follows: to determine the cause of deactivation in an acidic environment; to modify the titanium reactor system to obtain near total conversion; and to determine what happens to these model compounds after processing without the catalyst.

A series of experiments were performed with glycerol in H_2SO_4, $KHSO_4$, H_2O and KOH at 240 °C to determine the outcome of the feed material without the presence of the catalyst. One percent solutions of glycerol, methanol, and ethylene glycol were loaded into a Teflon lined Parr bomb. The reactor was heated to 240 °C, held for 4 hours, then cooled and the liquid mixture was analyzed by GC/MS. From this data, it was determined that in pure water, the feedstocks were stable and no by products were formed. In H_2SO_4, all of the glycerol had reacted to form byproducts, including large poly-ols, indicating dehydration and polymerization was occurring. The $KHSO_4$ data demonstrated that much of the glycerol was intact, with minor production of polymerization byproducts. In the alkali environment, over 50% of the glycerol was converted into byproducts, including organic acids and alcohols, with no evidence of polymerization. This data gives further evidence that base

catalyzed hydrolysis may be the better approach for hydrogen production. With glycerol, it avoids likely char precursors and condensing polymerization materials, as well as the corrosion issues acidic environments pose. Thus, the alkali environment is effective at hydrolysis of the raw material while avoiding detrimental pathways.

As a follow up to this result, UTRC's titanium reactor was fitted with Teflon coated rare earth magnetic stir bars and a magnetic stir plate was retrofitted to sit under the reactor, enabling stirring. Baseline experiments were performed on glycerol in water to determine whether the new reactor system was reproducible and if complete conversion could be obtained. Experiments were performed at 240 °C with 1 g of 0.5% Pt/Al_2O_3 and >90% conversion of glycerol was achieved with a good first order kinetic fit to the data. These experiments were repeated with WGS based catalysts, Pt and Pt-Re/$Ce_{0.5}Zr_{0.4}W_{0.1}O_2$, to compare the activity of these catalysts to the commercial Pt/Al_2O_3, as shown in Figure 10. **The addition of 1 wt% Re to the catalyst boosts the catalytic activity per gram of catalyst by a factor of four.**

The Pt-Re catalyst was selected for an investigation into the reforming of glycerol, ethylene glycol, and methanol in H_2SO_4, $KHSO_4$ and KOH. In summary, no reaction occurred with H_2SO_4 with any feedstock. Since methanol does not undergo condensation polymerization reactions, verified by GC/MS, the mechanism for deactivation must be a combination of side reactions and catalyst deactivation. SEM/EDS analysis of the used catalyst revealed severe leaching of cerium as well as sulfur contamination. $KHSO_4$ solutions exhibited limited activity and minimal leaching of materials was observed, but the surface was heavily contaminated by sulfur and potassium. There was significant activity with the Pt-Re/$Ce_{0.5}Zr_{0.4}W_{0.1}O_2$ catalyst in KOH solutions, yielding over 45% conversion before deactivation based on hydrogen evolution. The effluent gas concentrations are given in Figure 11. The negligible CO_2 production can be explained by in situ scrubbing by KOH. The first order hydrogen production rate constant was 3.6×10^{-5} $mL.g^{-1}.s^{-1}$, which is close to the reaction rate constant value in water of 4.4×10^{-5} $mL.g^{-1}.s^{-1}$. These were promising results as the reaction rate was high and the catalyst did not deactivate immediately. As the project progressed and additional analytical work was performed, it was determined that much of the observed "deactivation" was in fact side reactions forming organic acids.

After the model compound work was performed, the experimental program focused on the reforming of cellulose, hemicellulose, and lignin components obtainable from commercial sources, as well as mixtures thereof, to further understand the mechanism of CO and H_2 production in basic solutions. Synthetic wood ash in the form of potassium carbonate was investigated as an alternate to KOH as a hydrolysis agent. Once these experiments, described in Section 2.4, were completed, the project focused once again on using wood as a feedstock.

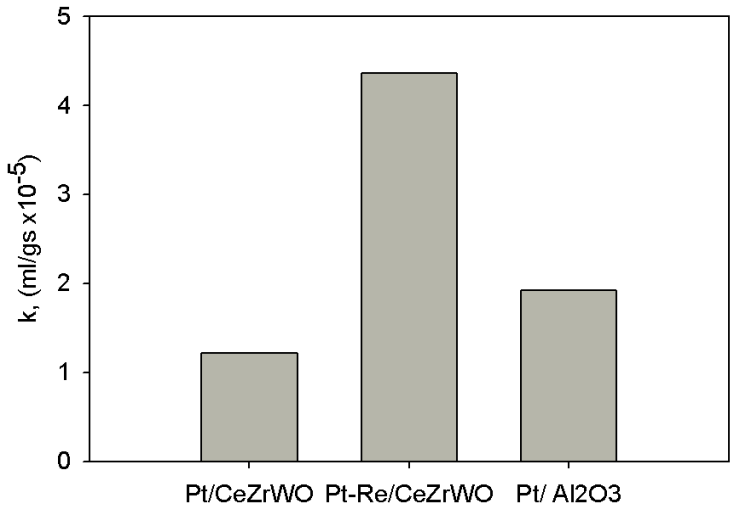

Figure 10: First order hydrogen production rate constants for the conversion of 1% glycerol at 240 °C with 1 g of platinum loaded catalysts.

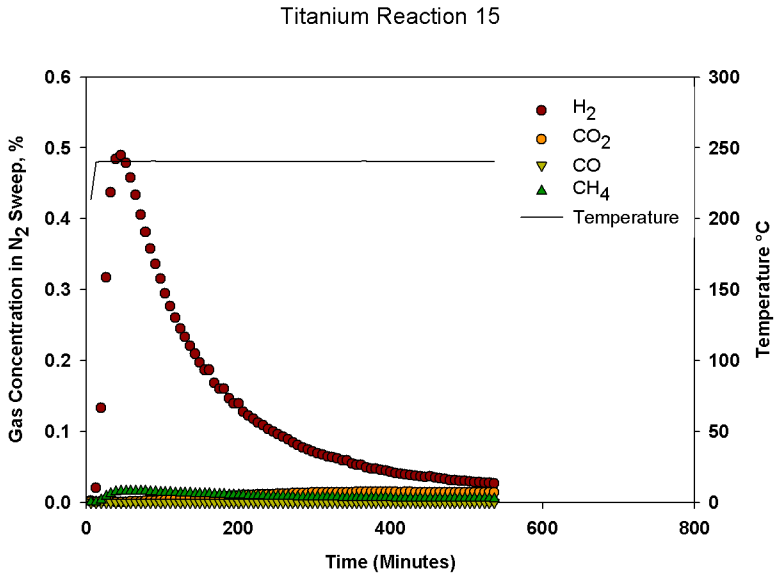

Figure 11: Effluent gas concentration for the aqueous phase reforming of 1 wt% glycerol in 0.2 M KOH solution at 240 °C with 1 g of Pt-Re/$Ce_{0.5}Zr_{0.4}W_{0.1}O_2$ catalyst.

2.2.4 Hydrogen Production from Yellow Poplar under Basic Conditions with Precious Metal Catalysts

Following the successful results of hydrolysis and reforming of biomass components, experiments were performed on raw biomass. Untreated yellow poplar (*Liriodendron tulipifera*) was obtained and processed into a fine sawdust. The wood was oven dried overnight and kept sealed to prevent moisture uptake. TGA analysis was performed on the dried wood, and it was determined that a residual 5% moisture was present, along with a total ash content of 1.1%. Based on values in the literature [6], the composition of yellow

poplar used for calculations was 43.9% cellulose, 15.3% hemicellulose, 26.0% lignin, and 14.4% uronic acid with 0.4% ash. For the analysis of the experiments presented here, the hemicellulose, cellulose, lignin and uronic acid were taken as reformable material, and used for mass balances. The cellulose was assumed to be $(C_6H_{10}O_5)n$, the hemicellulose was $(C_5H_8O_4)n$, the uronic acid was $(C_6H_8O_6)n$, and the lignin was $(C_8H_8O_3)n$.

Initial experiments with raw biomass feedstock were performed with 2 wt% yellow poplar in 0.1M K_2CO_3 with 2%Pt–1%Re/$Ce_{0.55}Zr_{0.45}O_2$. A temperature ramp was performed to determine whether there was activity and if there were any onset temperatures. The results are given in Figure 12 and Figure 13. It was evident that there was reforming activity on raw biomass throughout the entire temperature range. The activity increased with increasing temperature, but steadily declined at each temperature set point, likely due to hydrolysis limitations. The increase in CO_2 emissions at 240–260 °C was due to the release of CO_2 from K_2CO_3. In addition to H_2, the main byproduct was CH_4, which increased in concentration with increasing temperature. The reaction also produced small quantities of ethane and propane at increased temperature, indicating side reactions leading to byproducts may detract from the H_2 selectivity at higher temperatures. The total conversion was 41% with a selectivity of 88%, with a dark brown liquor remaining.

These results indicated that even without optimized hydrolysis and reforming conditions, significant conversion and reasonably good selectivity can be achieved using raw biomass. To test the limits of conversion in the system, a reaction was run at 310 °C with 1 wt% yellow poplar and stopped after 20 hours. The effluent concentration profiles are given in Figure 14. Significant H_2 and CO_2 were produced initially, followed by a significant tail of slow H_2 production. This suggested the reaction mechanism was very similar to that observed during microcrystalline cellulose and xylan experiments (described in Section 2.4). Overall conversion was 95% based on H_2 with a selectivity of 71%. The high conversion indicated that not only did the cellulose and hemicelluloses convert, but also the lignin, which was unexpected. The resultant solution was colorless, with some corrosion residues, as shown in Figure 15. The experiment was repeated with a similar conversion and selectivity (99% and 74%, respectively). Both internal analysis and two independent outside analytical labs confirmed that the solution only contained trace amounts of formic and acetic acids, further supporting the high conversions indicated by the material balances on the reactor system.

The overall energy conversion from the raw yellow poplar to gaseous products was calculated (see Table 5) assuming the LHV of dry yellow poplar was 18 MJ/kg. Therefore, for an initial charge of 0.5 g yellow poplar, 9 kJ of energy exists for conversion. With an overall H_2 selectivity of 74%, over 75% of the total energy from the dry wood is converted into H_2. The remainder of the energy is found in the lower order hydrocarbons, which could be used for heating of the reactor system.

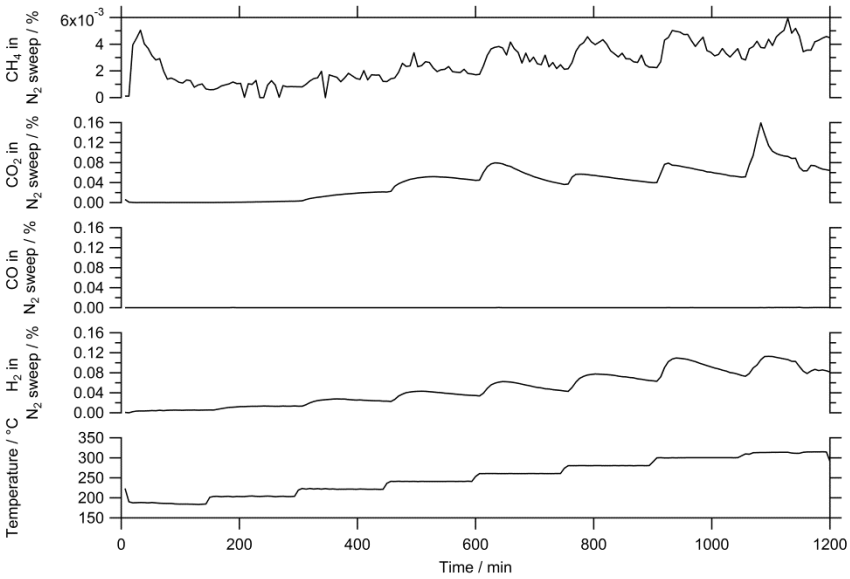

Figure 12: Hydrolysis and Liquid Phase Reforming of 2 wt% yellow poplar in 0.1M K_2CO_3, 0.5 slpm N_2 sweep gas, 1 g 2% Pt–1% Re/$Ce_{0.55}Zr_{0.45}O_2$.

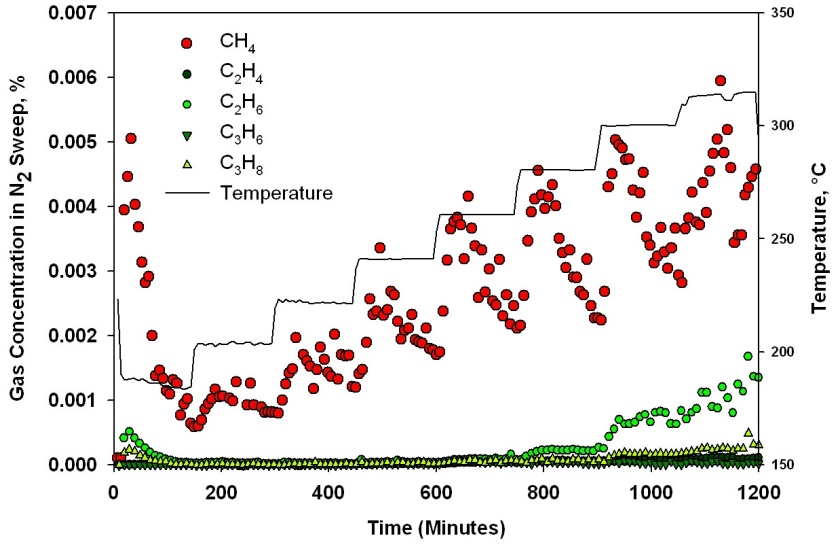

Figure 13: Hydrocarbon effluent profiles from the hydrolysis and Liquid Phase Reforming of 2 wt% yellow poplar in 0.1M K_2CO_3, 0.5 slpm N_2 sweep gas, 1 g 2% Pt–1% Re/$Ce_{0.55}Zr_{0.45}O_2$.

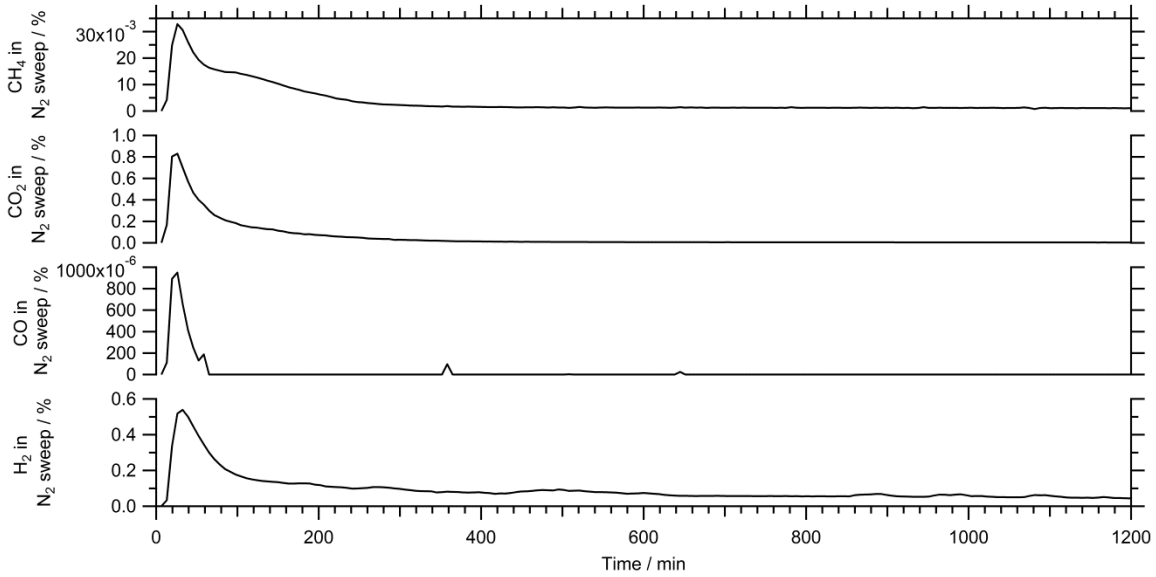

Figure 14: Effluent product profiles from the hydrolysis and Liquid Phase Reforming of 1 wt% yellow poplar at 310 °C in 0.1M K_2CO_3, 0.5 slpm N_2 sweep gas, 1 g 2% Pt–1% Re/$Ce_{0.55}Zr_{0.45}O_2$.

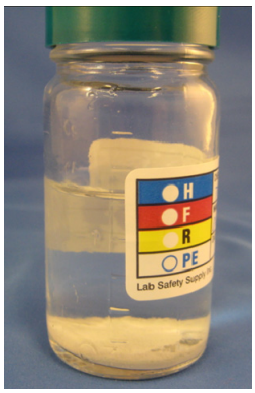

Figure 15: Reaction liquor obtained from the hydrolysis and Aqueous Phase Reforming of 1 wt% yellow poplar at 310 °C in 0.1M K_2CO_3, 0.5 slpm N_2 sweep gas, 1 g 2% Pt–1% Re/$Ce_{0.55}Zr_{0.45}O_2$. (The white solid is potassium titanate.)

Table 5: Energy conversion of 1% yellow poplar at 310 °C in 0.1M K_2CO_3, 0.5 slpm N_2 sweep gas, 1 g 2% Pt–1% Re/$Ce_{0.55}Zr_{0.45}O_2$.

	Hydrogen	Methane	C2s	C3s
Energy content / [MJ/kg]	121	50	47.8	46.35
Mass / g	5.59×10^{-2}	1.91×10^{-2}	7.59×10^{-4}	9.68×10^{-4}
Energy / kJ	6.763	0.953	0.036	0.045
%LHV in gas	86.74	12.22	0.47	0.58
%LHV from dry wood	75.15	10.59	0.4	0.5

2.2.5 Non-Purge Autoclave Testing with Precious Metal Catalysts

At this point in the project, nearly 100% conversion of 1 wt% yellow poplar had been reproducibly achieved with a Pt-Re/$Ce_{(1-x)}Zr_xO_2$ based catalyst in a custom built titanium reactor. Approximately 75% selectivity towards H_2 was achieved with an energy recovery of 75% based on the LHV of yellow poplar. Unfortunately, some corrosion products were evident in the reactor in the form of potassium titanate. The probable major source of this was caustic attack on the titanium screen used to hold the catalyst. Since this attack results in the formation of two moles of H_2 per mole of Ti attacked, the need to move to a corrosion resistant flow reactor was apparent. A new corrosion resistant reactor was built out of Zircadyne 702 and commissioned for wood and surrogate testing as described in Section 2.3.

During the course of the flow reactor work the question was raised as to whether it was possible to obtain high H_2 yields without the use of a sweep gas to remove the reactive species, or if hydrogenation and hydrogenolysis might consume the desired product H_2. To answer this question, a matched set of experiments was performed in a 2 L zirconium autoclave reforming 5 g yellow poplar in 1 L 0.1M K_2CO_3 with 10 g PtRe/$CeZrO_2$ at 310 °C for 12 hours, varying whether the reactor had a sweep gas passing through the system or not. Images of the reaction liquors and a summary table are given in Figure 16 and Table 6. Both solutions were clear and colorless, with trace organics found in solution (trace acetic and formic acid). Less hydrogen and carbon were observed in the gas phase of the closed vessel experiment. The reduced gaseous carbon production was likely due to the enhanced sequestering ability of the closed experiment, while the reduced hydrogen yield appeared to be due to organic acid production. However, the selectivity of the closed vessel experiment was slightly higher than the open vessel experiment.

These results indicated that a sweep gas was not required for near complete reforming of wood. In addition, these experiments were performed on a larger scale. This was an important step in beginning to understand whether scale up complexities would impact the project. Due to the amount of catalyst used in the runs, it was decided to re-use the catalyst during these runs. For example, the catalyst used in the closed vessel experiment had already survived 48 hours of reforming conditions. Although not conclusive, this was further evidence that the catalyst could have a long, stable life under reaction conditions.

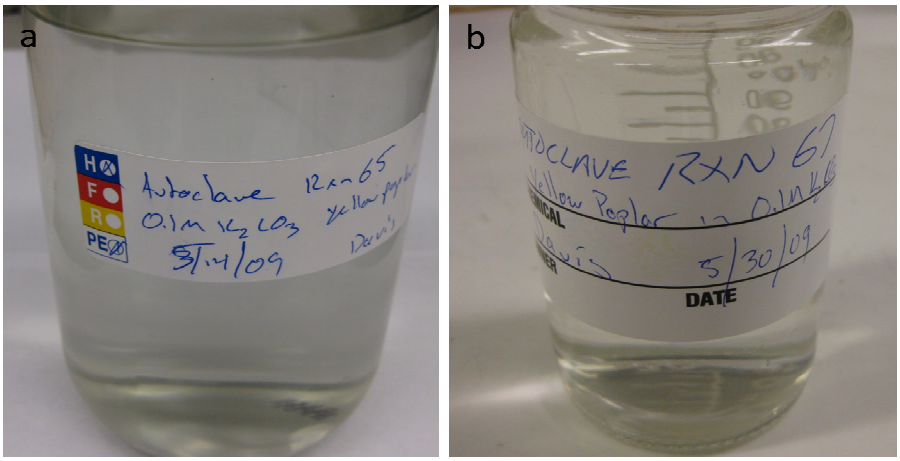

Figure 16: Reaction liquors from hydrolysis and liquid phase reforming of yellow poplar (a) with 0.5 slpm N_2 sweep gas and (b) in a sealed vessel, 5 g yellow poplar, 1 L 0.1M K_2CO_3, 10 g PtRe/$CeZrO_2$ at 310 °C for 12 hours.

Table 6: Comparison of results from Hydrolysis and LPR of yellow poplar with and without 0.5 slpm N_2 sweep gas, 5 g yellow poplar, 1 L 0.1M K_2CO_3, 10 g PtRe/$CeZrO_2$ at 310 °C for 12 hours. Conversion based on initial C and H content of the wood.

	Total moles collected		Conversion		H Selectivity
	C	H	C	H	
Sweep Gas	0.09	0.43	48%	135%	66%
Sealed Reactor	0.03	0.29	14%	92%	69%

2.2.6 Initial Hydrogen Production from Wood under Basic Conditions with Base Metal Catalysts

Following the precious metal catalyst experiments showing that a sweep gas was unnecessary for full reforming, the project moved to testing the possibility of liquid phase reforming with alternative catalysts. Raney Ni and Raney Co were purchased from Aldrich, both in 20-50 μm slurry form. Closed vessel reactions were performed identical to the reactions described in Section 2.2.5, except for the use of ≈10 g Raney catalysts. Pictures of the reaction liquors as well as a summary table are given in Figure 17 and Table 7.

Raney Ni performed well for the reforming of hydrolyzed wood. A clear and colorless reactor solution was obtained after 12 hours. However, as expected with nickel, significant methanation occurred, driving the H_2 selectivity down to 16%. On the other hand, Raney Co did not reform all of the hydrolyzed wood, but yielded a H_2 selectivity of 94%. These results were considered promising as an increase in selectivity positively affects system efficiency. In addition, a base metal catalyst such as cobalt would be significantly less expensive than a precious metal one, decreasing overall costs.

Significant effort was spent using Raney Co as a substitute reforming catalyst, particularly during the testing of surrogate compounds in a flow reactor (see Section 2.3). The benefits of using such a catalyst are its commercial availability in the appropriate fixed bed morphology and its significantly lower price. The initial results using Raney Co in a flow reactor with an ethanol feed at 310 °C were promising, showing steady H_2 production with 90% selectivity to H_2. The overall gas production rates were lower than the PtRe catalyst as expected. However, more detailed characterization of the liquid products was performed using an HPLC equipped with a refractive index detector. The HPLC analysis indicated that the ethanol was being converted into acetic acid with trace formic acid production. This result suggested that Raney Co does not effectively catalyze C-C bond cleavage in the ethanol, and simply oxidizes the ethanol to acetic acid, producing hydrogen.

The Energy & Environmental Research Center (EERC) of the University of North Dakota (UND) conducted experiments focused on the reforming of hybrid poplar with potassium carbonate and Raney Co. The testing of 5 wt% biomass using cobalt at temperatures of 300 °C and 330 °C resulted in generation of clear liquids, but gas production was minimal. Before learning of cobalt's inability to catalyze the C-C bond cleavage of ethanol, attempts to determine the cause of the low gas production included reducing the catalyst in situ and optimizing the stirring. **During wood reforming experiments, the cobalt catalyst favors organic acid formation and thus the dark product liquors as shown in Figure 17c. Based on the cobalt results, the base metal catalyst efforts were focused on nickel.**

Figure 17: Reaction liquors from hydrolysis and liquid phase reforming of yellow poplar with (a) PtRe/CeZrO$_2$, (b) Raney Ni, and (c) Raney Co; 5 g yellow poplar, 1 L 0.1M K$_2$CO$_3$, ≈10 g catalyst at 310 °C for 12 hours.

Table 7: Comparison of results from hydrolysis and LPR of yellow poplar in a closed vessel, 5 g yellow poplar, 1 L 0.1M K$_2$CO$_3$, ≈10 g catalyst at 310 °C for 12 hours. Conversion based on initial C and H content of the wood.

	Total moles collected		Conversion		H Selectivity
	C	H	C	H	
PtRe/CeZrO$_2$	0.03	0.29	14%	92%	69%
Raney Ni	0.08	0.38	42%	119%	16%
Raney Co	0.00	0.18	2%	57%	94%

2.2.7 Verification of Wood Reforming with Raney Ni in Different Batch Reactors with Hardwood Mixtures

To further verify the general reproducibility of liquid phase reforming of wood, a commercially available 100 mesh wood flour, shown in Figure 18, consisting of a mixture of hardwoods was used in several 2 L zirconium autoclave experiments. Two key experiments were performed where the base concentration was varied by an order of magnitude. For both experiments, a 5 wt% wood flour slurry was reacted at 310 °C and 120 atm (1800 psig) with a Raney Ni catalyst loading of 1 g catalyst per 1 g of wood. A low flow of N$_2$ was used to sweep the product gases out of the reactor and to the GC. KOH was used as the alkali source. One test was conducted with 0.2 M KOH and the other was performed with 2.0 M KOH. The effluent product profiles for hydrogen and methane from the reactor are shown in Figure 19.

Similar to previous experience, the experiment with 0.2 M KOH resulted in a clear, colorless product liquor (see Figure 20) and an approximate mass balance closure of 100%. Based on hydrogen yield and carbon conversion, the wood was essentially 100% converted to gas. However, the selectivity to hydrogen was only 15%, with more methane produced relative to hydrogen. For the 2.0 M KOH experiment, the hydrogen yield based on total reforming was lower, only 75%, with a selectivity to hydrogen of 60%. **These experiments showed that increasing the concentration of base for an unmodified Raney Ni catalyst results in higher levels of unreformable organic acids while increasing the gas phase selectivity from methane to hydrogen.**

Figure 18: Commercial 100 mesh wood flour.

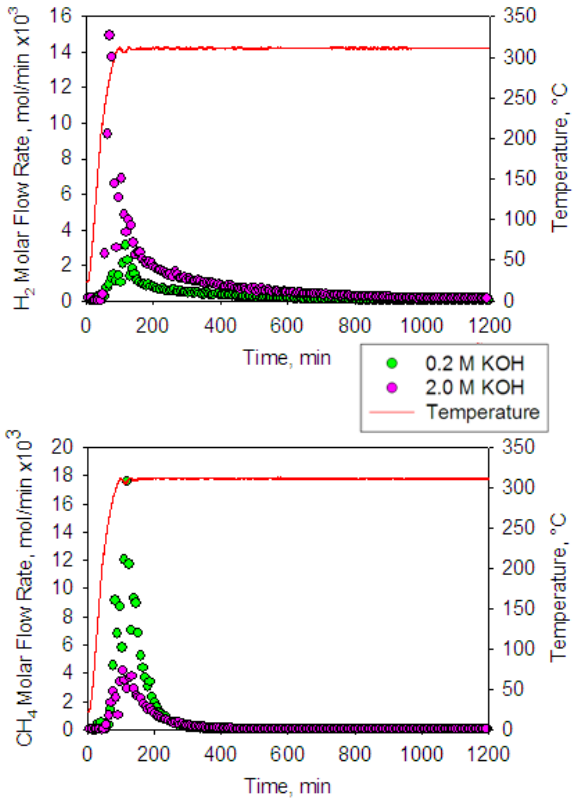

Figure 19: Effluent product profiles for hydrogen and methane from the hydrolysis and liquid phase reforming of 5 wt% 100 mesh wood flour with Raney Ni and 0.2 M KOH at 310 °C.

Figure 20: Reaction liquor from hydrolysis and liquid phase reforming of 5 wt% 100 mesh wood flour with Raney Ni and 0.2 M KOH at 310 °C.

A batch reactor experiment was carried out with wood to verify that the larger size powder form (40 µm to 90 µm particles) of Raney Ni catalyst used in some flow reactor experiments (see Section 2.3) worked as well as the 20-50 µm Raney Ni catalyst. The test was run with a 2% wood slurry and 0.2 M K_2CO_3 at 310 °C and 1500 psig. A total of 7 g of Raney Ni 2800 was used in the test. N_2 gas was used to sweep the product gases out of the reactor and to the GC. Similar to previous batch experiments with wood, 100% conversion of the wood was achieved with a H_2 selectivity of 72%. Figure 21 shows a picture of reaction liquor product which was a clear solution. The greenish powdery material visible in the picture was determined to be mainly nickel oxide plus trace amounts of other metals, such as Fe and Cr, which probably came from the Inconel reactor itself.

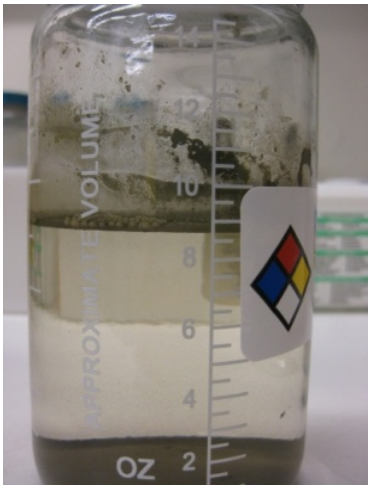

Figure 21: Reaction product liquor from wood reforming at 2% feed, 0.2 M K_2CO_3, 310 °C, 0.6 L min^{-1} N_2 sweep gas and 7 g Raney Ni.

2.2.8 Study of Impact of Base on Raney Nickel Liquid Phase Reforming of Wood

For the last year of the project, EERC's effort was focused on batch, single-step hydrolysis and reforming experiments. The experiments were performed using a standard, unmodified Raney Ni catalyst and potassium hydroxide base to further investigate the impact of base to wood ratio on H_2 yield and selectivity. All tests were completed in EERC's 7.6-L autoclave system with a constant wood concentration of 8 wt%. The test conditions for these experiments are given in Table 8.

The H_2 yield and H_2 selectivity results for the 21 experiments are shown in Figure 22 and Figure 23, respectively. Consistent with previous predictions from atomistic and thermodynamic modeling for ethylene glycol (see Section 2.5), as well as batch wood reforming experiments performed at UTRC, **increasing the base to wood ratio increased the selectivity of the process toward hydrogen production versus methane. However, the higher base levels decreased the H_2 yield, favoring organic acid formation over gas production.**

Table 8: Final test matrix for EERC base to wood batch reforming study.

Test Number	Wood Loading, wt fraction	Catalyst Loading, g Ni/g wood	Base Loading, g KOH/g wood	Temperature, °C
1	0.08	1	4.6	325
2	0.08	1	4.6	300
3	0.08	1	4.6	275
4	0.08	1	6.9	325
5	0.08	1	6.9	300
6	0.08	1	6.9	275
7	0.08	1	9.2	325
8	0.08	1	9.2	300
9	0.08	1	9.2	275
10	0.08	1	0.092	325
11	0.08	1	0.092	300
12	0.08	1	0.092	275
13	0.08	1	0.138	325
14	0.08	1	0.138	300
15	0.08	1	0.138	275
16	0.08	1	0.184	325
17	0.08	1	0.184	300
18	0.08	1	0.184	275
19	0.08	1	0.41	300
20	0.08	1	1.0	300
21	0.08	1	2.0	300

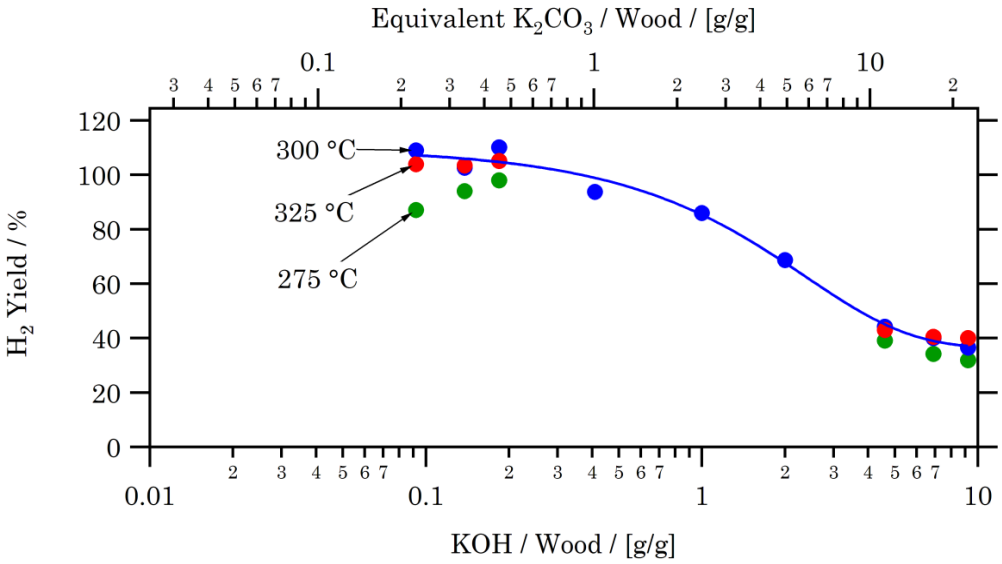

Figure 22: Impact of KOH to wood ratio on the H_2 yield with Raney Ni of 8 wt% hybrid poplar in a batch reactor. Also shown on the chart is the equivalent K_2CO_3 to wood ratio.

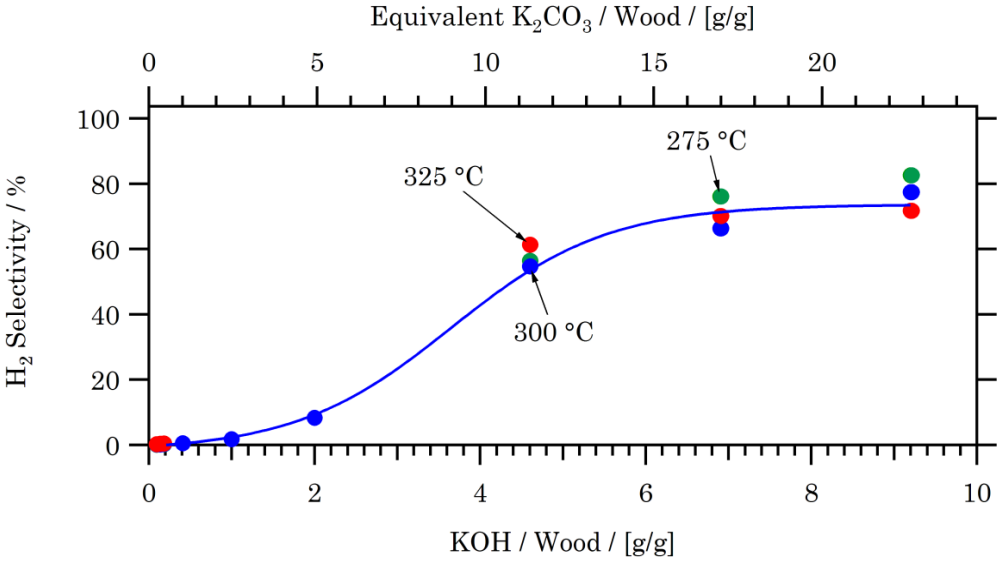

Figure 23: Impact of KOH to wood ratio on the H_2 selectivity with Raney Ni of 8 wt% hybrid poplar in a batch reactor. Also shown on the chart is the equivalent K_2CO_3 to wood ratio.

2.3 Liquid Phase Reforming in Flow Reactors

2.3.1 Flow Reactor for Investigation of Continuous Liquid Phase Reforming

As described in Section 2.2, model compounds, particularly glycerol, were used to investigate the impact of operating conditions on batch reactor systems. In particular, Section 2.2.5 noted the necessity of constructing a reactor to avoid the titanium corrosion

observed in the yellow poplar batch reactor experiments. Thus, to avoid reactor corrosion and to simplify kinetic studies, it was decided to move to a corrosion resistant flow reactor.

Significant effort was put forth to obtain information on what materials would be compatible with the reaction environment. Two materials that the literature details as resistant at these hot alkali conditions are zirconium and Inconel 625 (and a few other Ni based alloys). Due to the high nickel content of Inconel, a reactor with zirconium walls was chosen, more specifically, Zircadyne 702 (95% Zr, ~4% Hf, trace Fe, Ni). Zircadyne possesses the structural integrity necessary for the designed reaction condition range, along with inherent chemical inertness.

A schematic of the flow system is given in Figure 24. A high pressure Isco syringe pump (500D) was used to pump high pressure reactants. In addition to the liquid inlet, the system was set up to allow for inlet flows of H_2 as well as N_2. The reactor was constructed of a 20-in long Zircadyne 702 tube, 0.5-in OD with a 0.065 in wall thickness. The reactor lay inside a 10.5-in infrared furnace with approximately 3 in out of the bottom of the furnace and 9 in out of the top. Above the heated section, a 1-in OD stainless steel (SS) double tube condenser, approximately 5 in long, was affixed around the Zircadyne reactor. This condenser was sufficient to reduce the internal temperature to below 30 °C, well below the alkaline corrosion limit for 316 SS. The top and bottom of the reactor were affixed to the SS tubing system through a 0.5-in VCR fitting. An aluminum heating block was clamped onto the reactor tube within the furnace to ensure uniform heating of the reactor. A 0.25-in Zircadyne thermowell was constructed to slip down through the reactor into the heated zone for accurate tracking of the reaction temperature. A high pressure N_2 sweep gas was introduced after the reactor to minimize residence time in the exit piping and act as a diluent for gas production calculation. The temperature and pressure of the reactor effluent was measured and controlled by a Tescom ER3000 back pressure regulator (BPR). Upon depressurization to atmospheric pressure, the effluent passed through a gas-liquid separator, followed by a flow meter and GCs for analysis.

In order to reduce residence time as well as hold the catalyst in place, a packing material was needed. Due to the apparent stability of the UTRC $CeZrO_2$ catalyst, as well as the commercial availability of ZrO_2 grinding media of various sizes, yttria stabilized ZrO_2 was chosen as the packing material. A standard packing of the reactor shown in Figure 24 consisted of filling the bottom of the reactor, about 4 in into the heated zone, with 2-mm ZrO_2 beads. Above this, 0.5-mm ZrO_2 beads were used until the catalyst section, which was 75% of the distance to the top of the heated zone. The powdered catalyst was diluted with 0.5-mm ZrO_2 spheres to a catalyst packing density of 0.57 g cm^{-3}. On both sides of the catalyst, a few yttria stabilized ZrO_2 felt discs were used to hold the catalyst in place. The thermowell was set to rest just above the catalyst zone. The remainder of the top of the reactor (the annulus of the reactor and the thermowell) was filled with 0.5-mm ZrO_2 beads.

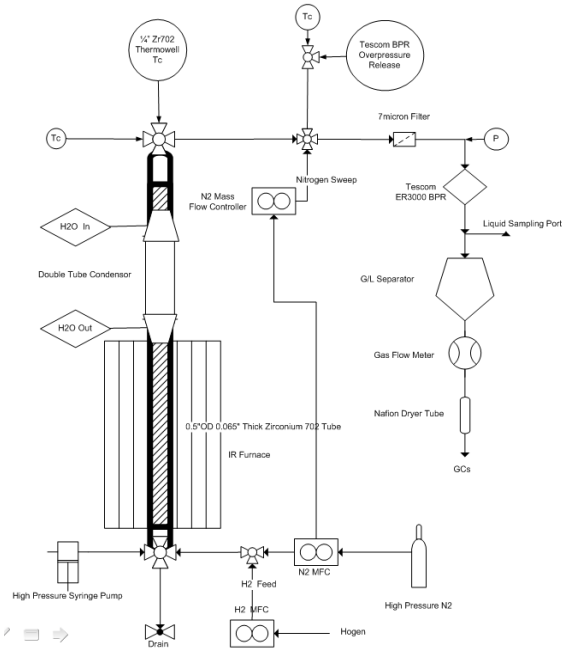

Figure 24: Flow reactor setup.

2.3.2 Ethanol Reforming under Basic Conditions

The initial test of the reactor consisted of using 1 g 1.5% Pt-1.2% Re/$Ce_{0.65}Zr_{0.35}O_2$ with 1 wt% ethanol as the feedstock. The reactor was operated at temperatures of 250 °C, 280 °C, and 310 °C at a pressure of 1640 psi with a reactant liquid flow rate of 1 mL min^{-1} and a N_2 sweep gas flow rate of 0.3 L min^{-1}. Effluent molar flow rates and carbon conversions are given in Figure 25. At each temperature, the effluent molar flow rates were stable, and increased with increasing temperature. This indicated that the catalyst and reaction bed is likely stable under these conditions and that the catalyst would not be swept away by the reaction mixture. The conversion increased with increasing temperature, with a calculated activation energy for the formation of H_2 of 54 kJ mol^{-1}. The reaction selectivity towards H_2 was 48%, 46%, and 48% at each subsequent temperature step, with CH_4, and to a lesser degree C_2H_6, being the main byproducts of the reaction.

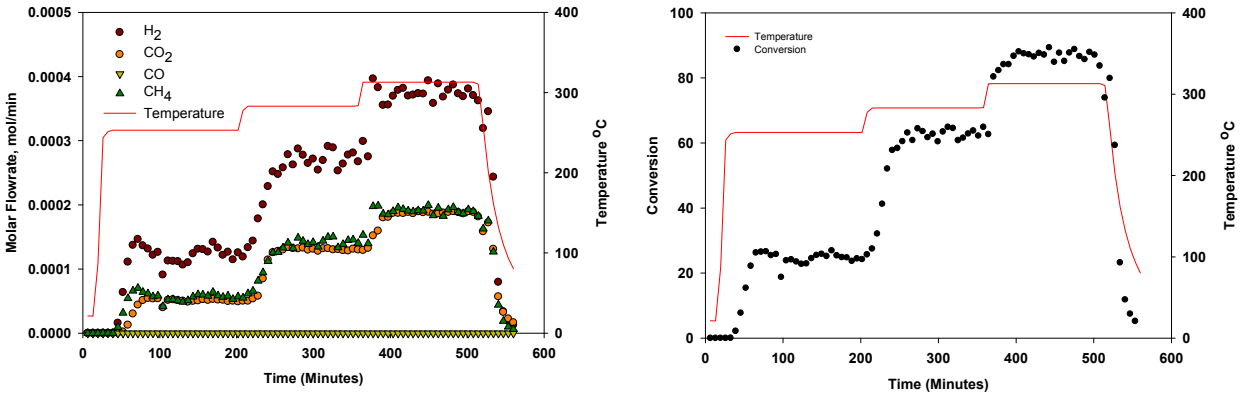

Figure 25: Liquid phase reforming results for 1 wt% ethanol with 1 g 1.5% Pt-1.2% Re/$Ce_{0.65}Zr_{0.35}O_2$ with a feed flow rate of 1 mL min^{-1} and a sweep gas flow rate of 0.3 L min^{-1}, at 1640 psi.

Subsequent experiments in the flow reactor were performed with 1.7 wt% ethanol in 0.1M K_2CO_3 to determine how the system behaves in the presence of base. The reactor was run at 250 °C, 280 °C, and 310 °C with a liquid feed flow rate of 2 mL min^{-1}, shown in Figure 26, and 3 mL min^{-1}, given in Figure 27. For both flow rates, the reaction gas production increased with increasing temperature. Both flow rates produced H_2 as the main product with CH_4 being the major byproduct. CO_2 was only noted at higher temperatures due to the CO_2 scrubbing effect of K_2CO_3. More than a saturation level of CO_2 must be generated before any CO_2 will be observed in the gas phase. The H_2 selectivity of the system varied depending on the temperature. The selectivities were 46%, 48%, and 65% at 2 mL min^{-1} and 41%, 51%, and 71% at 3 mL min^{-1} for 250 °C, 280 °C, and 310 °C, respectively. At 3 mL min^{-1}, the reactor was allowed to run for over 200 minutes at 310 °C to determine the effect of time on stream. Little degradation in H_2 production was noted during the experiment (the large dip in H_2 production was due to the reactor being taken off line for refilling of the syringe pump).

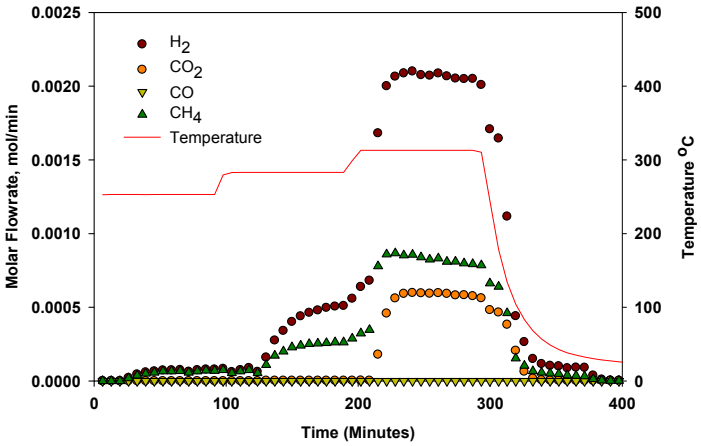

Figure 26: Effluent molar flow rate of gas during the liquid phase reforming of 1.7 wt% ethanol in 0.1 M K_2CO_3 with 1 g 1.5% Pt-1.2% Re/$Ce_{0.65}Zr_{0.35}O_2$, at a feed flow rate of 2 mL min^{-1} and a sweep gas flow rate of 0.3 L min^{-1} at 1640 psi.

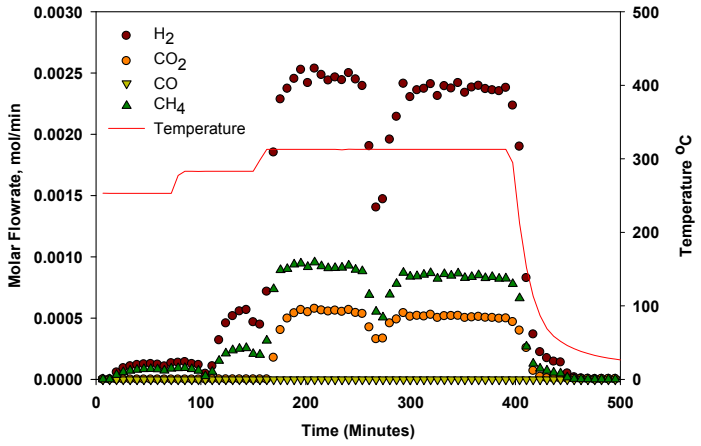

Figure 27: Effluent molar flow rate of gas during the liquid phase reforming of 1.7 wt% ethanol in 0.1 M K_2CO_3 with 1 g 1.5% Pt-1.2% Re/$Ce_{0.65}Zr_{0.35}O_2$, at a feed flow rate of 3 mL min^{-1} and a sweep gas flow rate of 0.3 L min^{-1} at 1640 psi.

Upon dissecting the reactor after the reactions, it was found that the inert packing had lost its structural integrity and become a powder. More importantly, the beads used as a diluent for the catalyst also lost their integrity, encapsulating the catalyst particles as if in a cement plug. This may have been detrimental to the reaction kinetics of the system and prevented high conversions.

With the data obtained from the liquid phase reforming of ethanol in the presence of base, a network of reactions to describe the system was derived. In addition to the main reaction products of H_2 and CO_2, only CH_4, C_2H_6, and C_3H_8 byproducts were detected in any appreciable quantities. This reaction network led to the development of rate equations and a kinetic model for a plug flow reactor used to estimate the rate constants. Parameter estimation techniques were used to fit the ethanol data to the model. Figure 28 shows the model prediction and experimental data points for the liquid phase reforming of ethanol in 0.1M K_2CO_3 at 310 °C. It was evident that the reaction network adequately described the reforming of ethanol at the conditions studied. It was thus possible to use this network to determine optimal conditions and required bed length for high conversion. The approach should also be applicable to more complicated systems, including the liquid phase reforming of raw biomass.

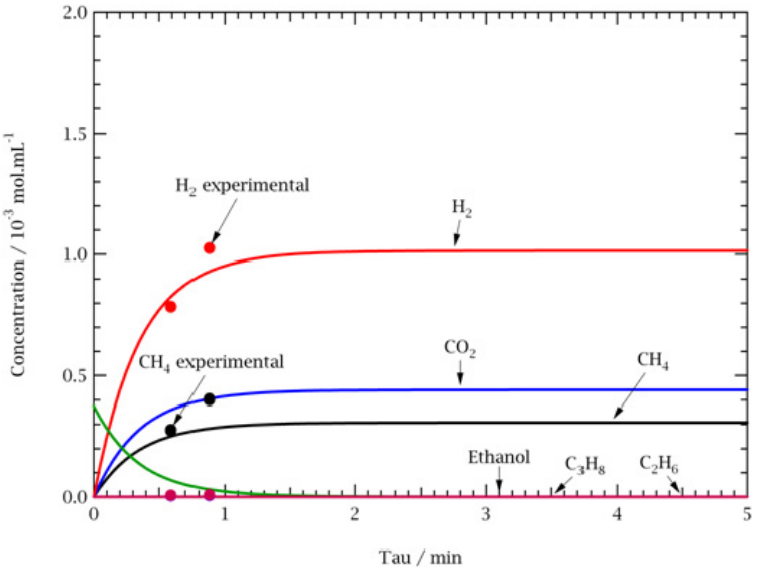

Figure 28: Model prediction and experimental data for the liquid phase reforming of ethanol at 310 °C in 0.1M K_2CO_3 as a function of residence time (tau) in the flow reactor.

2.3.3 Hydrolyzed Woody Biomass Reforming

Attempts to used pre-hydrolyzed biomass as the feed to the reforming reactor proved much more difficult than ethanol, as the degradation of the inert packing thwarted all efforts to gather data. Dissolution studies were carried out in a batch high pressure bomb to determine whether acceptable inert materials could be identified. Dissolution studies were carried out at 310 °C for 12 hours. Pictures of several of the materials before and after processing are given in Figure 29. CaO/HfO_2 stabilized Zr as well as the previously used yttria stabilized Zr exhibited significant degradation during the processing. Several other materials showed significant promise, including rutile TiO_2, Ce stabilized ZrO_2, and SiC.

Rutile TiO_2 was used as the next inert packing due to its availability. 1 wt % yellow poplar was hydrolyzed in the zirconium autoclave in 0.2M KOH at 310 °C for 10 hours. The

hydrolyzed solution was filtered to remove residual solids (approximately 1.2% solids recovered from original solid loading). After hydrolysis and filtration, it was noted that a solution left out at ambient conditions or in a refrigerator continued to precipitate solids. This was an important observation, as these tar-like solids may be catalytically more difficult to deal with than the precursors which led to their formation. These precursors are likely highly active lignin fragments that may be best reformed immediately following their production, before they react with each other to form the observed tar-like solids.

The solution of hydrolyzed yellow poplar was flowed over a 2 g bed of 1.5% Pt-1.2% $Re/Ce_{0.65}Zr_{0.35}O_2$ chunks (~4-mm square) mixed with crushed rutile TiO_2 pellets. The total bed volume was 4 cm^3. The flow of hydrolyzed yellow poplar was set at 1 mL min^{-1} and the reactions carried out at 310 °C. Unfortunately, significant chromatography issues arose, due to plugging of downstream valves and lines. Data could not be gathered and extensive system repair and redesign was required.

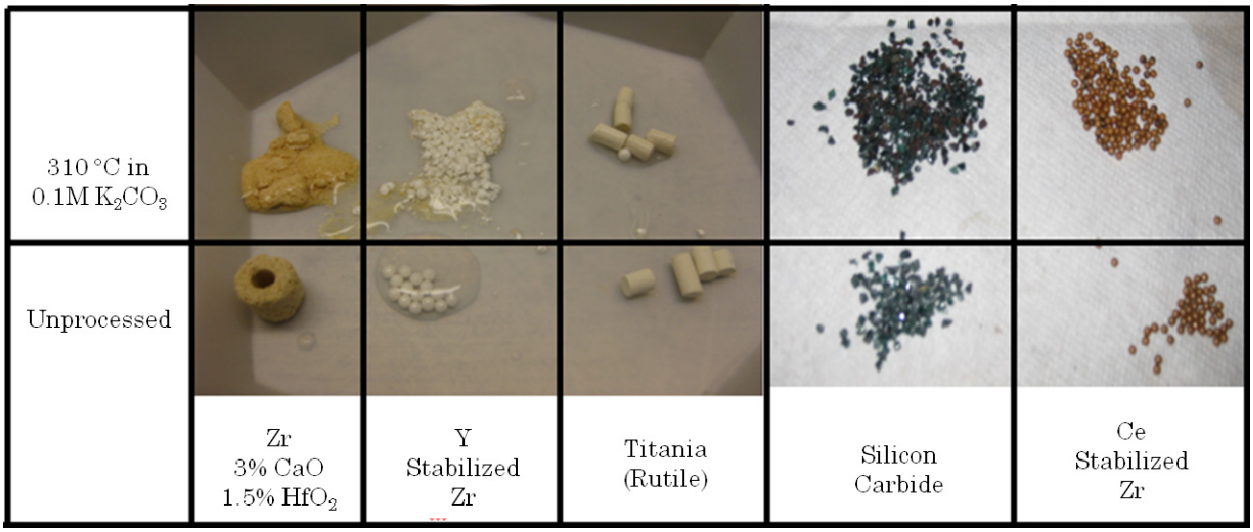

Figure 29: Visual results for dissolution studies on various inert packing materials.

A new inert packing, ceria stabilized zirconia, was identified and obtained. To determine the feasibility of reforming wood in a flow reactor, the reactor was packed with a 2" bed of 2 g $PtRe/CeZrO_2$ catalyst with 1 g yellow poplar below the catalyst. The idea was that as the wood was hydrolyzed, it would be carried into the catalyst region by the liquid flow, and subsequently be reformed. The reaction was performed at 310 °C at 1700 psi. A schematic of the flow setup as well as the effluent profiles are given in Figure 30 and Figure 31. The overall conversion of the wood into the gas phase was calculated to be 25% for hydrogen and 20% for carbon (not including sequestered CO_2).

Overall, the results were promising; indicating that hydrolysis and reforming of yellow poplar over PtRe is possible in a flow system. However, having raw wood packed into the flow reactor is not practical. Although the experimental setup avoided the issue of whether a pre-hydrolyzed solution could be cooled and then pumped through the reaction zone without significant, detrimental changes in composition, it was likely the biomass underwent insufficient hydrolysis before reaching the catalyst bed. In addition, this result raised questions as to whether it was possible to obtain high H_2 yields without the use of a sweep gas to remove the reactive species, or if hydrogenation and hydrogenolysis may consume the desired product. The batch experimental work described in Section 2.2.5 was

performed to show that hydrolysis and liquid phase reforming in an autoclave can be achieved without a sweep gas.

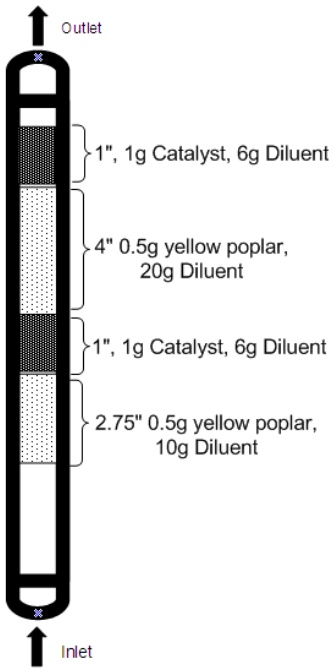

Figure 30: Schematic of wood hydrolysis and reforming flow reactor.

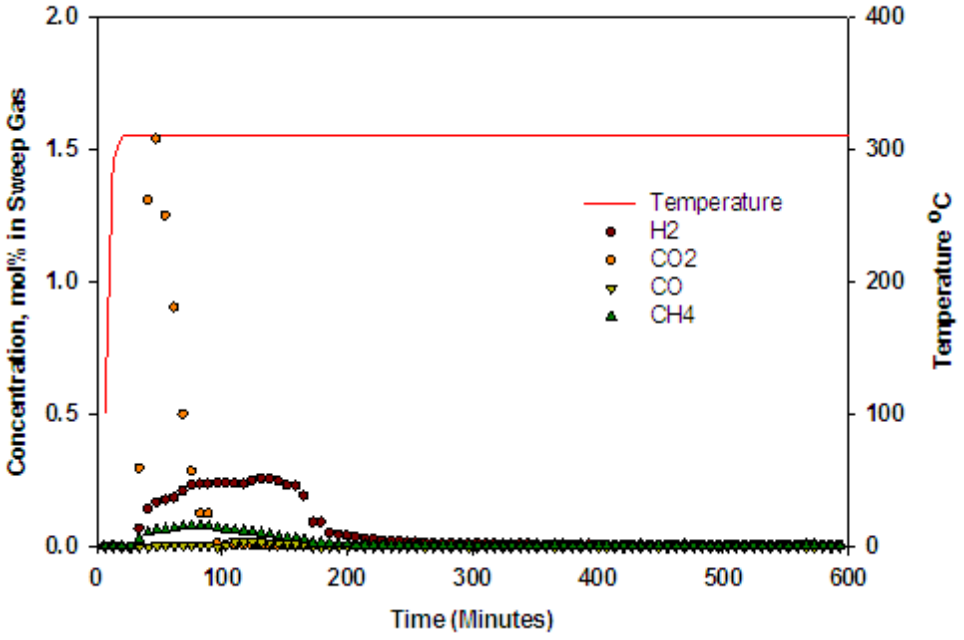

Figure 31: Effluent concentration profile for hydrolysis and LPR of yellow poplar over PtRe/CeZrO$_2$ in flow reactor, 0.1M K$_2$CO$_3$ at 0.5 mL min^{-1}, 310 °C.

2.3.4 Additional Model Compound Reforming under Basic Conditions

Following the successful demonstration of the near 100% conversion of wood to hydrogen-containing gas using liquid phase reforming (LPR) in a batch autoclave, the project efforts were focused on further understanding the durability and kinetics of the process in a plug flow reactor system. Model compounds, such as ethanol and 1,4-butanediol were used to study a fixed bed reactor system using UTRC's Pt-Re based catalyst. Tests showed that the catalyst could reform the model compounds for periods greater than 250 hours without signs of degradation.

Significant effort was put into determining the kinetics and durability of reforming catalysts in a plug flow reactor system. The reactor tube was loaded with 0.25 g $PtRe/CeZrO_2$ with Ce stabilized Zr grinding media as a diluent to a total catalyst bed volume of 1.8 mL. Liquid phase reforming experiments were performed on the catalyst with feeds of 1% ethanol in H_2O with and without the addition of 0.1M K_2CO_3. The reactions were performed at temperatures of 250 °C to 310 °C. The product molar flow rates are given in Figure 32. In segment A, 1% ethanol in water exhibited a steady production of hydrogen with a relatively moderate selectivity of about 0.55 (defined as moles H in H_2 divided by total moles H in product gas). The solution was switched to 1% ethanol in 0.1M K_2CO_3 for segment B. The CO_2 production dropped as expected due to the scrubbing effect of the alkali. The H_2 production rate dropped by a factor of 3.5, while the CH_4 production rate dropped by a factor of ~20. This led to an increase of H_2 selectivity to 87%. Data was gathered at flow rates of 2–5 mL min^{-1} at various temperatures and then the feedstock was switched to 1,4 butanediol in 0.1M K_2CO_3 and then back to ethanol in 0.1M K_2CO_3. The selectivity to H_2 from 1,4 butanediol was nearly 100% as virtually no CH_4 was produced. Switching back to ethanol brought the system back to where it had been. No measurable deactivation was observed throughout the entire 230 hour experiment. The low conversions that were observed in these experiments rendered efforts to develop a kinetic model unsuccessful.

In order to gather data for the development of a kinetic model, a larger catalyst bed was necessary, so that changes in temperature and flow rate would more significantly influence conversion. In addition, the higher conversion would enable higher H_2 molar flow rates, enabling the validation of the feasibility of coupling a liquid phase reforming system to a palladium membrane for H_2 separation. A $1^9/_{16}$" bed comprised of 2 g $PtRe/CeZrO_2$ was established in the plug flow reactor. A 1 wt% solution of ethanol in 0.1M K_2CO_3 was flowed through the reactor at flow rates between 3 and 6 mL min^{-1} at 310 °C. After stabilization at the prescribed temperature and flow rate, the system was held for at least an hour to collect the data and then the flow rate was changed to the next set point. Between flow rates, the syringe pump needed to be refilled and the reactor cooled. Unfortunately, during the restart from a weekend downtime, the pressure drop built up in the reactor tremendously indicating plugging in the catalyst bed. To return to normal flow, the reactor needed to be drained and dried by flushing with hot N_2. This brought the pressure drop back down to a manageable level, but the activity of the system had dropped by at least 15%. Later dissection of the catalyst bed showed cementing of the catalyst bed which likely caused bypassing of a majority of the active catalyst. **This result indicated an issue with the morphology of the PtRe catalyst. The morphology of the catalyst needs to be optimized for liquid phase fixed bed reactor testing.**

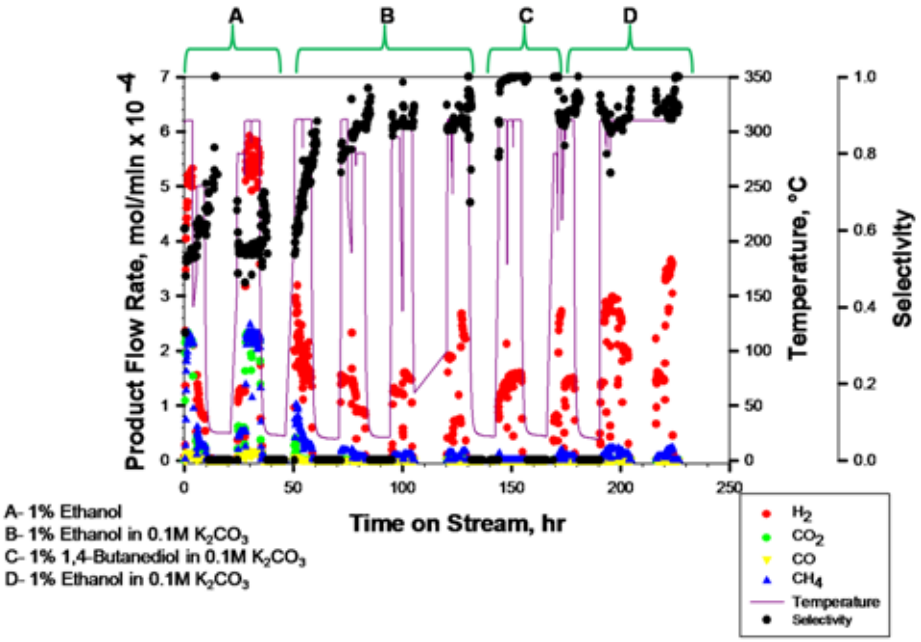

Figure 32: Durability plot for PtRe/CeZrO$_2$ catalyst for the reforming of ethanol and 1,4-butanediol.

2.3.5 Demonstration of Continuous Production of High Purity Hydrogen

Although the plug flow reactor bed could not be used for kinetic studies, it could be used for demonstration of the reforming coupled with a palladium membrane. A 10% ethanol in 0.1M K_2CO_3 solution was flowed through the reactor bed at 310 °C at 3 mL min^{-1}. The nitrogen sweep gas was turned off to maximize H_2 concentration in the effluent stream. The effluent gas stream from the reforming reactor was approximately 213 mL min^{-1} and composed of approximately 64%H_2. The effluent gas stream was fed to a palladium-copper alloy membrane held at 450 °C at a pressure of 193 psig. The system was allowed to run for 45 minutes to stabilize and collect data. The data from the experiment is given in Figure 33. The system behaved as expected, with a 93% H_2 recovery, indicating maximum recovery of the H_2 from the reformate gas stream.

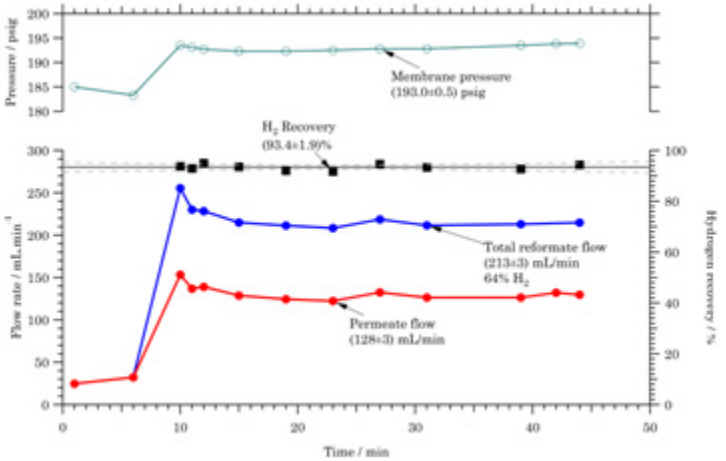

Figure 33: Experimental results for hydrogen separation with a Pd alloy membrane from liquid phase reformed ethanol over a PtRe/CeZrO$_2$ catalyst.

2.3.6 Flow Reactor Testing with Raney Cobalt Catalysts

As part of the goal of reducing catalyst costs, and thus capital costs, the project focused on transitioning from a precious metal based catalyst to one with base metal as the active component. Significant effort was spent using Raney Co as a substitute reforming catalyst. The benefits of using such a catalyst are its commercial availability in the appropriate fixed bed morphology and its significantly lower price. Initial results using 1.5 g Raney Co in the reactor at 310 °C were promising, showing steady H_2 production with 90% selectivity to H_2. The overall gas production rates were lower than the PtRe catalyst as expected.

In order to get kinetic data, a new reactor was built with 4.5 g Raney Co to get sufficient conversion to enable kinetic modeling. A 1% ethanol solution in 0.1M K_2CO_3 was flowed through the reactor at 250 °C, 280 °C, and 310 °C at flow rates of 3–6 mL min^{-1}. Data for the reaction at 310 °C is given in Figure 34. The effluent profiles exhibited stable H_2 production at each flow rate. Increasing the flow rate generated more H_2 and slightly reduced the CH_4 production.

An aliquot of the liquid effluent was collected at each set point and analyzed by HPLC equipped with a refractive index detector. The HPLC analysis indicated that the ethanol was being converted into acetic acid with trace formic acid production. This result suggests that Raney Co does not effectively catalyze C-C bond cleavage in the ethanol, and simply oxidizes the ethanol to acetic acid, producing hydrogen. Although this confirms cobalt is not a sufficient reforming catalyst, it does leave the door open for the use of it as a potential catalyst support. It is base tolerant and has both sufficient surface area and very good thermal conductivity. Raney Co's demonstrated oxidation of alcohols may be helpful in the hydrolysis process.

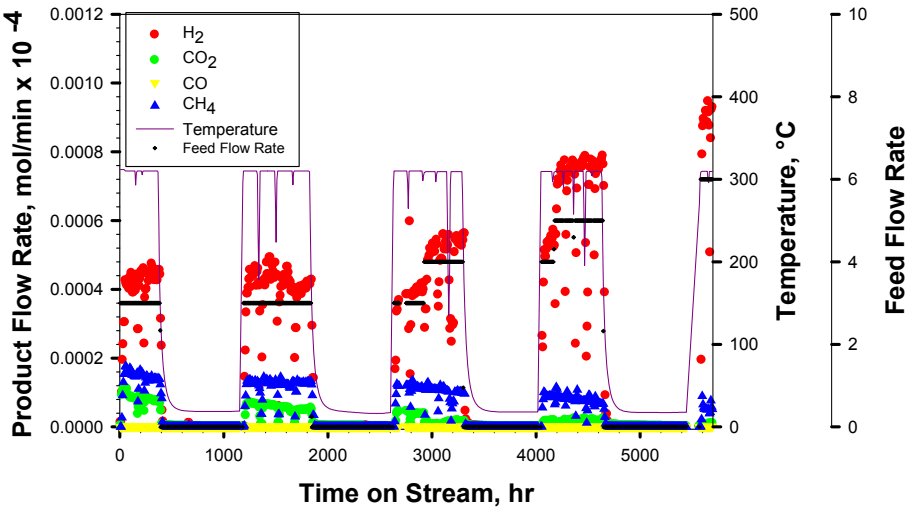

Figure 34: Effluent molar rates from liquid phase reforming of 1% ethanol in 0.1M K_2CO_3 with 4.5 g at 310 °C.

2.3.7 Flow Reactor Testing with Ethylene Glycol to Investigate Acid Formation During Reforming

Based on the results from the Raney Co tests, further investigation of the reforming of ethanol over PtRe/$CeZrO_2$ revealed that a majority of the ethanol was also being oxidized in the system to acetic acid and small amounts of formic acid. Further experimentation with Raney Co confirmed the same mechanism, that the C-C bond cleavage may not have been

the preferred catalytic pathway, and that the oxidation of the molecule appeared to dominate.

It was hypothesized that one of the factors controlling the H_2 production and acid production was the fact that ethanol contained a non-oxygenated carbon. Flow reactor experiments were then performed with a feed of ethylene glycol and the effect of base type and base concentration were investigated over a $PtRe/CeZrO_2$ catalytic bed. Data for H_2 conversion is given in Figure 35. H_2 conversion is defined as the total atomic H in the gaseous species divided by the total maximum H_2 possible by complete reforming. In this calculation, it is assumed that the methane was formed by CO (or CO_2) methanation. Therefore, the H_2 lost to the production of water by methanation is added back in to more accurately reflect the total conversion. As shown in Figure 35, liquid phase reforming (LPR) of 1% ethylene glycol in 0.2 M KOH at 310 °C topped out at ≈60% conversion. Longer residence times did not drive the reaction further. Increasing the temperature to 330 °C also had little effect on the overall H_2 yield. However, increasing the base concentration to 0.7 M and subsequently 2.0 M KOH significantly increased the H_2 yield by over 20%.

Liquid HPLC analysis of the reaction liquors confirmed the depletion of ethylene glycol in the system and revealed the presence of organic acids in the product at the lower base concentrations. These organic acids have been shown to be very stable in high temperature aqueous environments, partially explaining the maximum attainable hydrogen yield. At higher base concentrations, the concentration of these byproducts was significantly less. In addition to increasing the overall H_2 yield, the selectivity to H_2 increased as the base concentration increased.

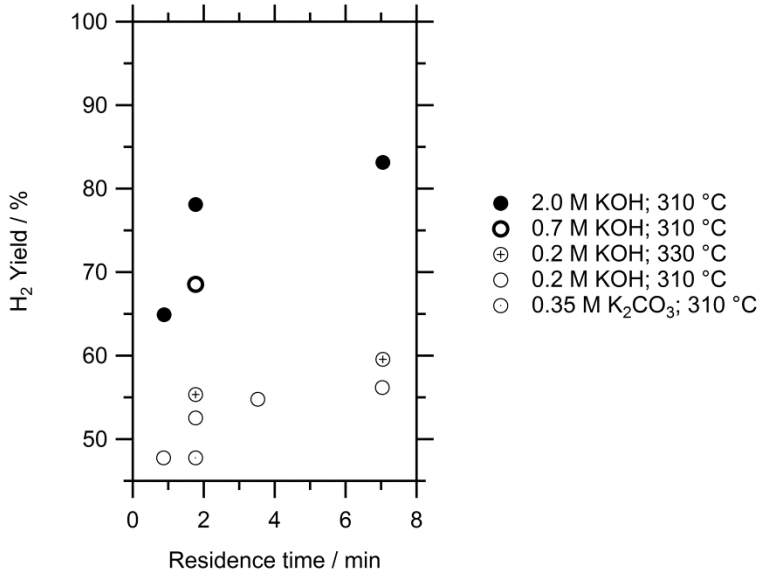

Figure 35: Liquid phase reforming of 1 wt% ethylene glycol over a 1 g bed of $PtRe/CeZrO_2$ at 1780 psig.

These results were not in line with those observed in a batch reactor. Previously, 99% conversion of sawdust to gaseous species was possible with small concentrations of base. Only trace levels of organic acids remained after reaction. **The flow reactor is fundamentally different for several reasons, including residence time, mixing, pH variations, and product gas concentrations. The data seen in Figure 35 suggested that a high pH level must be maintained during the reaction to continue to drive it forward.**

2.3.8 Flow Reactor Testing with Raney Nickel

These results suggested that an inexpensive base metal catalyst would be capable of performing the reaction and that byproducts could be tailored by base concentration. Furthermore, this may also indicate that the traditional liquid phase reactions of oxygenated hydrocarbon with water may be substituted by a base reaction with the oxygenate, minimizing the possibility of side reactions occurring. To validate this hypothesis, a reactor was loaded with 4 g of Raney Ni and a series of flow reactor tests were performed with 5 wt% ethylene glycol to determine the effect of different bases and strength of base.

The hydrogen yield data is given in Figure 36 and the selectivity given in Figure 37. Similar trends were observed with Raney Ni as with PtRe. Regardless of the concentration used, the overall H_2 yield was identical for all KOH cases. The K_2CO_3 data appeared to have slower kinetics and significantly lower selectivity. **All alkaline cases demonstrated higher yields than runs with only pure water. Furthermore, by tailoring the base concentration, selectivity was improved on a known methanation catalyst.** This may either be due to an increased ability to absorb CO_2 and thus remove it from the reactant pool, or, more likely, the base reacts with CO to form H_2 and K_2CO_3, and thus higher concentrations will improve the shift kinetics and lower the methane concentration.

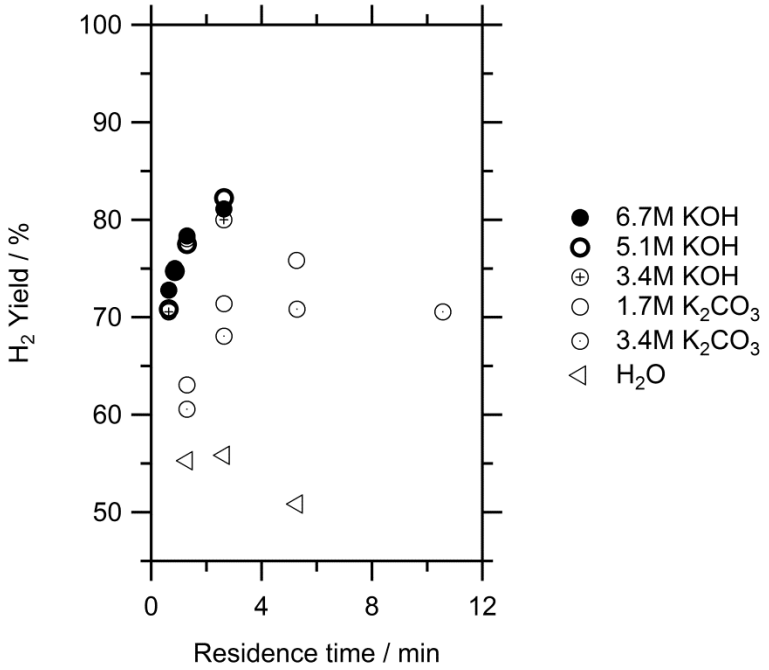

Figure 36: H_2 yield for LPR of 5 wt% ethylene glycol over a 4 g bed of Raney Ni at 1780 psig and 310°C.

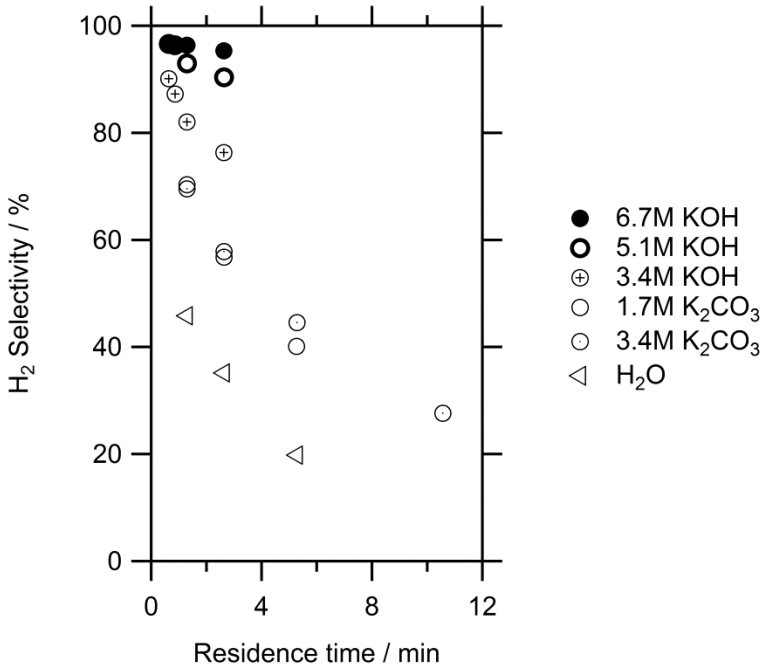

Figure 37: H_2 selectivity for LPR of 5 wt% ethylene glycol over a 4 g bed of Raney Ni at 1780 psig and 310°C.

2.3.9 Flow Reactor Testing with Modified Raney Ni to Improve Performance

The effect of base concentration on the liquid phase reforming of ethylene glycol indicated that increased base concentration drove the reaction, producing a higher H_2 yield. Moreover, the high concentrations of base inhibited methanation reactions traditionally observed in reforming using Ni or other base metal catalysts. A thermodynamic analysis of the system indicated that with significant KOH levels, reforming to produce H_2 was more favorable than methanation, contrary to traditional liquid phase reforming. However, when looking at overall system design, using KOH to drive the reaction and inhibit CH_4 was offset by the energy intensive regeneration of KOH, as it was converted to K_2CO_3 and $KHCO_3$ in the reaction. Therefore, the team needed to devise a way to use K_2CO_3 or $KHCO_3$ as the alkaline catalyst and still enable highly efficient and selective conversion of the surrogate feedstock using an inexpensive catalyst.

To accomplish this task, either a different catalyst was required, one which had little methanation activity, or the nickel catalyst had to be modified to suppress the methanation reaction. The team attempted to modify the nickel based catalyst due to the known ability of Ni to promote liquid phase reforming as well as the fact that most non-precious metal catalysts capable of breaking C-C bonds have significant methanation activity. The Raney Ni catalyst was doped with small amounts of a promoter and the activity was studied in the flow reactor. Experiments were performed at 310 °C with a 2.5% feed of ethylene glycol in various bases. The yield and selectivity data is given in Figure 38 and Figure 39. For comparison, the data for unmodified Raney Ni at 1.7 M K_2CO_3 is also shown.

The modification of Raney Ni with a small percentage of a promoter significantly improved the selectivity to H_2 by severely reducing methanation reactions. Unlike unmodified Ni, a very high KOH concentration was not necessary to maintain high selectivity after doping, removing the requirement of

an energy intensive KOH regeneration system and allowing the use of K_2CO_3 as the base. Moreover, this data shows the reforming reaction may be inhibited by CO_2 or more specifically, carbonate ions. With the modified Raney Ni, increasing K_2CO_3 concentration subsequently decreased yields. Without an active methanation catalyst, CO_2 was at a much higher concentration in the system than in the unmodified case, leading to a higher selectivity, but lower overall conversion.

For all base concentrations, the yield appeared to hit a maximum near 80%. HPLC analysis of the reaction mixtures revealed only formic acid (potassium formate) as a byproduct. Some aldol products, such as 2-butanone, were seen in a GC/MS of the effluent liquid.

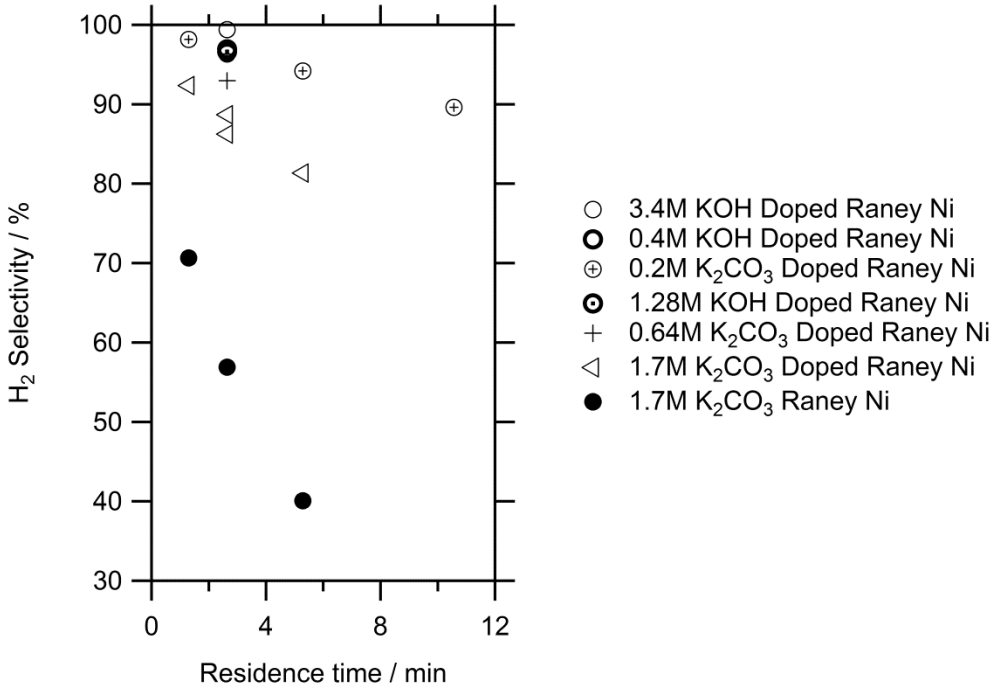

Figure 38: H_2 selectivity for LPR of 2.5 wt% ethylene glycol over an 8 g bed of doped Raney Ni at 1780 psig, 310 °C.

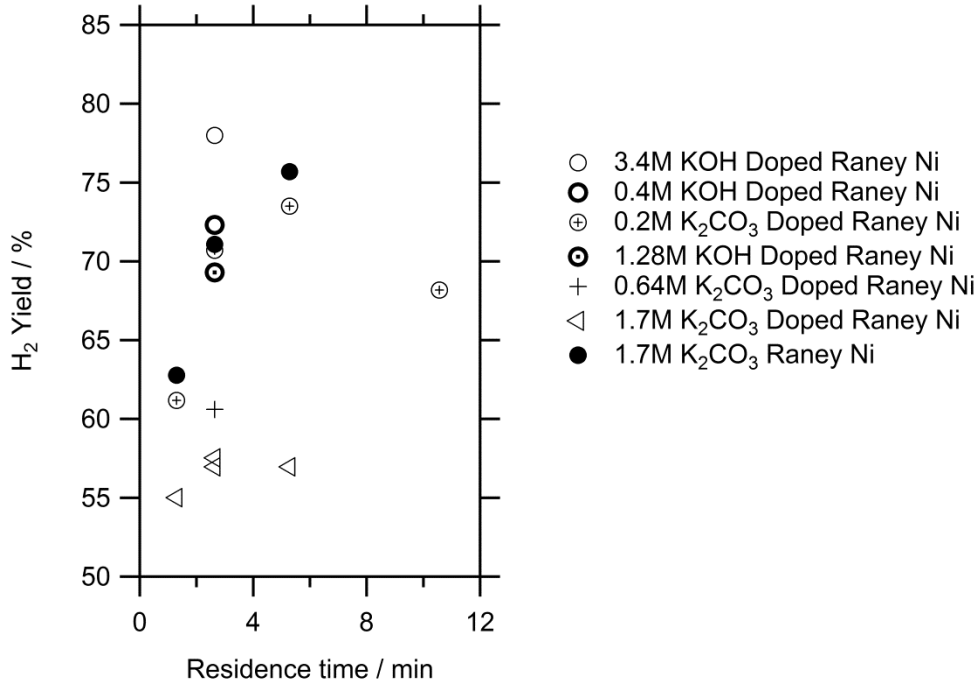

Figure 39: H_2 yield for LPR of 2.5 wt% ethylene glycol over a 8 g bed of doped Raney Ni at 1780 psig, 310 °C.

2.3.10 Flow Reactor Testing by Co-feeding Catalyst and Wood

To properly size the equipment, particularly the reactor, for a demonstration unit, as well as increase understanding of liquid phase reforming of a complicated feed mix, experimental efforts were focused on reforming raw biomass in the small flow reactor rig. A small flow rate is needed (2–5 mL min^{-1}) to reach the residence times estimated for the reforming reaction. In addition, reaction time must be allowed for the hydrolysis reaction, so even lower flow rates may be needed. Several attempts to feed the flow reactor with UTRC's slurry pump failed. The primary reason was that the size of the bore in the pump head was too great to keep the pulverized wood entrained, leading to wood dropping out of solution and clogging the check valves.

An alternate experimental setup was devised, which entailed the indirect pumping of wood slurry into the flow reactor. The schematic of the apparatus is given in Figure 40. A solution of wood in water was stored in a high pressure autoclave with a head pressure of N_2. The fixed bed reactor was pre-pressurized to the desired pressure with water and a base solution was introduced via a syringe pump for the desired flow rate of base. When the system was stable, the autoclave pressure was raised to match the fixed bed reactor, and a valve was opened to allow material to begin flowing from the dip tube in the stirred autoclave to the fixed bed reactor. High pressure N_2 was introduced into the autoclave through a mass flow controller. With constant pressures and temperatures, the flow rate of wood slurry to the fixed bed reactor could be calculated from the volumetric flow rate of pressurized gas into the autoclave.

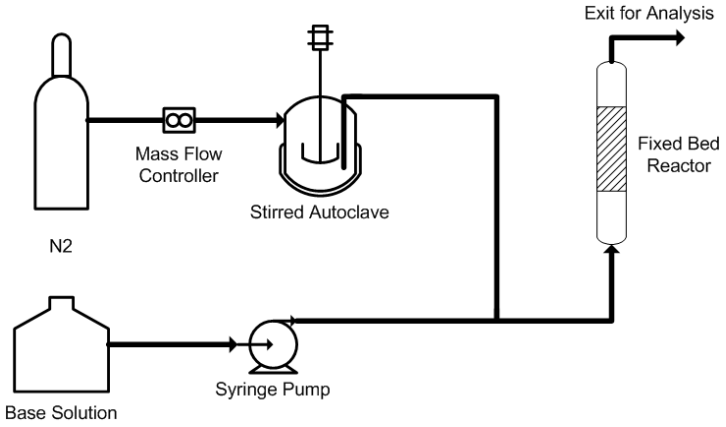

Figure 40: Schematic of indirectly pumped biomass slurry flow system.

Initial testing commenced after troubleshooting this setup to ensure the delivery of wood slurry to the reactor. In order for a demonstration unit to function properly, it was necessary to determine the minimum residence time necessary to hydrolyze/liquefy the wood. An empty reactor was installed where the fixed bed reactor would normally be and a 2.5 wt% wood mixture was introduced at a flow rate of 5 mL min^{-1} with sufficient base to produce a 0.2M K_2CO_3 solution. The system ran for 60 minutes at 310 °C and a brown liquid was observed coming out of the reactor. The wood was sufficiently hydrolyzed at this flow rate, corresponding to a 4.5 min residence time. The system was restarted at 10 mL min^{-1} with sufficient base to equal 0.2M K_2CO_3, but some plugging was observed in the system. Therefore, a residence time of 5 minutes for hydrolysis was used for fixed bed reactor testing.

The empty reactor was replaced with a fixed bed reactor comprised of a large open cavity below an 8-g bed of Raney Ni catalyst. The system was operated at 310 °C with a base concentration of 0.2M K_2CO_3 and a wood slurry flow rate of 3 mL min^{-1}. A brown solution was observed coming out of the reactor, but minimal gas was produced. A solution of ethylene glycol was subsequently pumped through the reactor, and significant levels of H_2 evolved, demonstrating the activity of the catalyst.

This result led to the hypothesis that the plug flow reactor was forming intractable compounds in the bulk phase before the catalyst had the opportunity to reform the compounds. This hypothesis would explain the difference in the batch and flow reactor results. Therefore, to test this hypothesis, Raney Ni slurry would be pumped with the wood into the reactor. As the wood heats up and the base depolymerizes the wood, a catalyst would be there to immediately reform the hydrolyzed compounds, creating gas. Unfortunately, the same issues encountered during pumping of the wood were exacerbated by the nickel, as its bulk density is about 7 g cm^{-3}.

To alleviate this, starch was added to thicken the solution and entrain the catalyst for pumping purposes. The starch would then be consumed in the process, but after it performed its task of carrying the catalyst and wood into the reactor. The technique of adding the starch would only be required for small scale testing, as the slurry pump had successfully demonstrated the ability to move the Raney Ni-wood flour slurry at higher flow rates.

Starch solutions were made up, and an aliquot of Raney Ni was added to determine the minimal concentration required for sufficient entrainment. Pictures of the solutions after a 5 min settling time are given in Figure 41. A 2% mixture of starch in water was sufficient to

entrain the catalyst for pumping via the slurry pump. This was verified by pumping at atmospheric pressure. In subsequent testing, the starch concentration was increased to 4%.

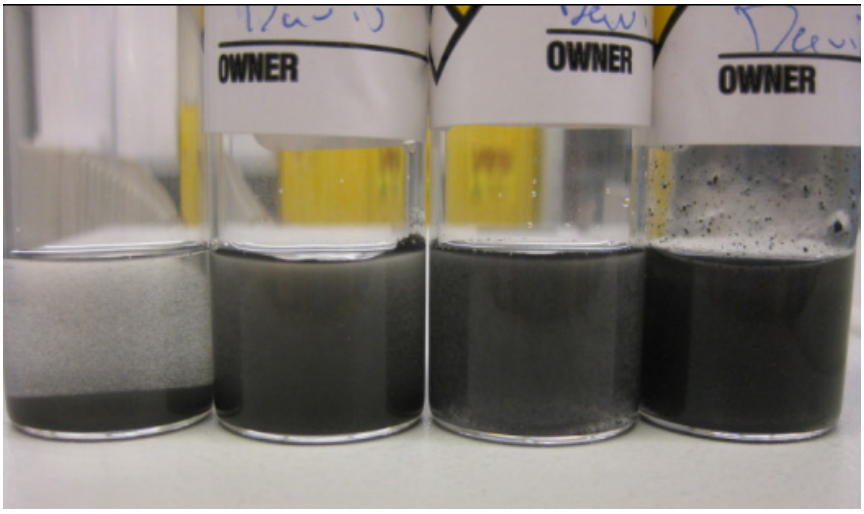

Figure 41: Raney Ni entrained in starch solutions after 5 minutes of settling time; from left to right 0 wt%, 0.5 wt%, 1 wt%, and 2 wt% starch.

After several troubleshooting experiments and changes to the experimental setup, two key experiments were performed to investigate the catalyst co-feed approach. In the first experiment, a 4 wt% starch solution with a standard Raney Ni catalyst was co-fed into the flow reactor. As the catalyst was not promoted, the experiment resulted in the production of H_2, CO_2, and methane from the starch, but there was more methane than hydrogen. The starch conversion at this residence time was low (on the order of 20%).

Based on the success of the first experiment, 2 wt% wood was added to a 4 wt% starch solution and co-fed with the catalyst in the flow reactor. There was an increase in the amount of H_2, CO_2, and methane produced for the same operating conditions (flow, pressure, and temperature). The conversion of feed material was on the order of 30% for this run. In addition, the product solution was brown in color and smelled similar to reacted wood products that have been previously observed. The increase in gas concentrations, color of the liquid effluent, and the odor of the product indicated that some or all of the wood was converted along with the starch.

In addition to the co-feed experiments, which were successful but resulted in very low conversions, additional packed bed experiments were performed using starch. However, significant geometry changes were required for the reactor setup to work, and the packed bed reactor system frequently plugged. It became apparent that mixing and high velocities to eliminate mass transfer issues may be critical to achieve high conversions and avoid organic acid side reactions. As a result, the reactor development effort shifted focus to a continuous stirred tank reactor (CSTR) configuration for wood and wood component testing (see Section 2.4).

2.4 Wood Component Testing in Batch and Stirred Tank Reactors

Due to the complexity of lignocellulosic biomass as well as the complicated chemical reactions occurring during base catalyzed hydrolysis and reforming, lignocellulosic components were investigated to determine optimal conditions for H_2 production. Based on

literature values for oven dried yellow poplar [6], lignocellulosic biomass is composed of cellulose (43.91 wt%), hemicellulose (15.27 wt%), lignin (25.97 wt%), uronic acids and other compounds (14.44 wt%) with 0.41 wt% ash. The previous swamp maple experiments, as well as the literature, led the team to believe that each of the components will have different activation temperatures with regard to the hydrolysis reactions, as well as the reforming reactions. Therefore, experiments were performed in a batch reactor with individual wood compounds: microcrystalline cellulose, xylan (as a hemicellulose surrogate), and low sulfonate lignin. Later, cellulose was tested in a continuous stirred tank reactor to further narrow down the reaction conditions for continuous operation in a demonstration system.

2.4.1 Wood Component Testing in Batch Reactor

Initial hydrolysis coupled with reforming reactions with microcrystalline cellulose and xylan were performed at 240 °C with 0.2M KOH. Information from the literature indicated that xylan hydrolysis would occur at a lower temperature than cellulose, and thus would have a faster rate and higher conversion at equivalent conditions. Lignin, due to its aromatic nature, should require higher temperature for reforming. Prior to running the reactions, it was necessary to confirm that a catalyst was needed to perform the desired reaction. In separate experiments, 1 wt% xylan, cellulose, and lignin were hydrolyzed in the presence of 0.2M KOH at 240 °C for 12 hours. For each case, less than 1% conversion to the gas phase resulted with total liquefaction of the feedstocks to a translucent brown to black liquor, as shown in Figure 42a and Figure 42c for lignin and cellulose, respectively. These experiments were repeated in the presence of 1 g of 2% Pt–1% Re/$Ce_{0.5}Zr_{0.4}W_{0.1}O_2$, with results listed in Table 9. Lignin experiments, which produced no gas during reforming, were not listed in the table due to the high sulfur content inherent to extracted lignin from the purification process, completely deactivating the catalyst. Lignin hydrolysis liquors were very dark brown to black with no solids.

For xylan and cellulose, the reaction liquors were brown to light brown and completely translucent. No solids were visible. In agreement with the literature, higher conversion of xylan over cellulose was achieved with identical conditions. At 240 °C, both feedstocks demonstrated a hydrogen selectivity of 85%, based on total H_2 produced verses total H_2 in all gaseous species. The reactions demonstrated a large initial burst of gas production, followed by a long tail of activity, shown in Figure 43. CH_4 was the major byproduct, with minimal higher order hydrocarbons.

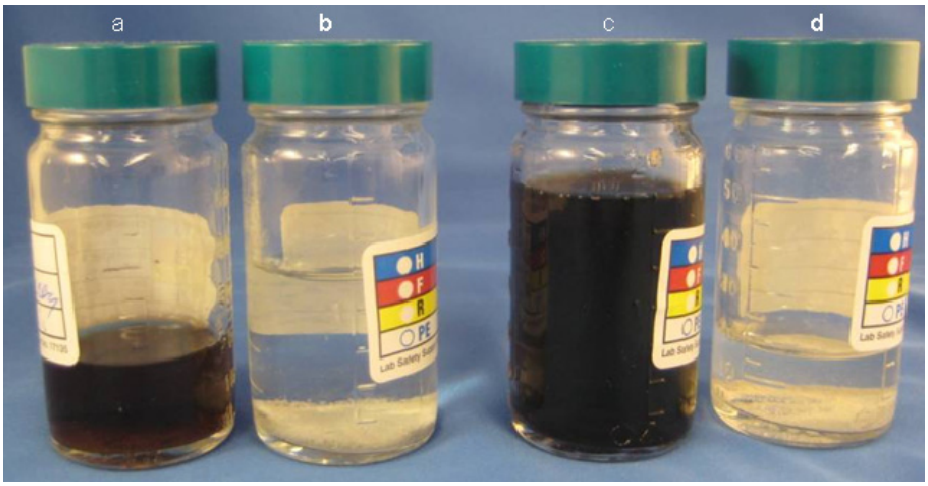

Figure 42: Reaction product liquors for xylan and cellulose hydrolysis and hydrolysis with reforming: (a) 1 wt% xylan, 0.2M KOH, 310 °C, 0.5 slpm N_2 sweep gas; (b) 1 wt% xylan, 0.2M KOH, 310 °C, 0.5 slpm N_2 sweep gas, 1 g 2% Pt–1% Re/ $Ce_{0.5}Zr_{0.4}W_{0.1}O_2$; (c) 1 wt% cellulose, 0.2M KOH, 310 °C, 0.5 slpm N_2 sweep gas; and (d) 1 wt% cellulose, 0.2M KOH, 310 °C, 0.5 slpm N_2 sweep gas, 1 g 2% Pt–1% Re/ $Ce_{0.5}Zr_{0.4}W_{0.1}O_2$.

Table 9: Results of hydrolysis coupled with Liquid Phase Reforming of 1 wt% feedstock in 0.2M KOH with 1 g of 2% Pt–1% Re/$Ce_{0.5}Zr_{0.4}W_{0.1}O_2$ and 0.5 slpm N_2 sweep gas.

	Temperature / °C	H_2 Conversion / %	H_2 Selectivity / %
Xylan	240	60	85
Microcrystalline Cellulose	240	24	85
Xylan	310	83	64
Microcrystalline Cellulose	310	72	89

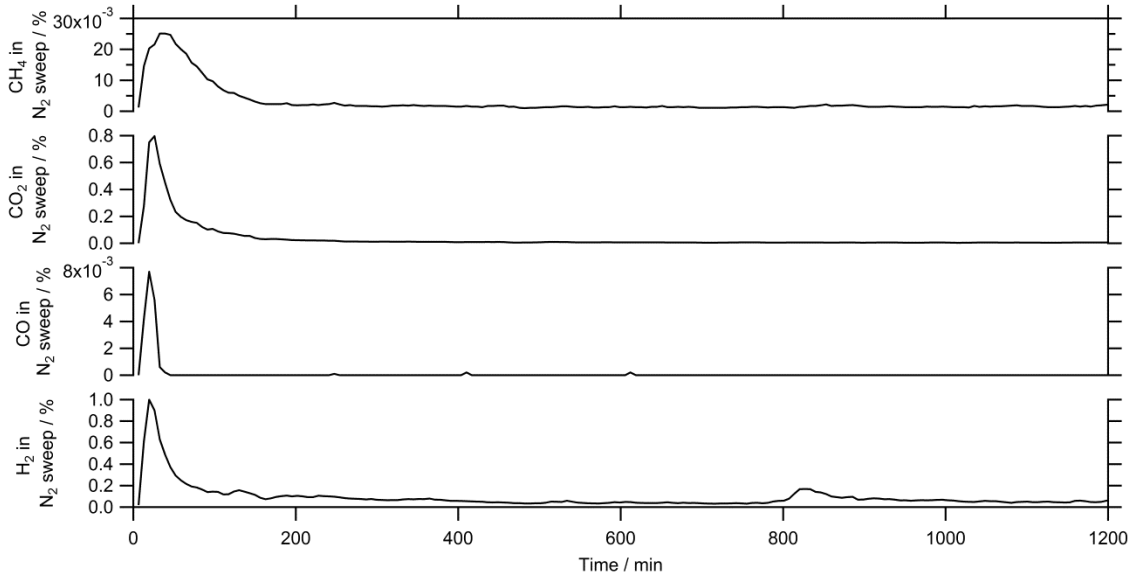

Figure 43: Effluent gas profiles from 1 wt% microcrystalline cellulose, 0.2M KOH, 310 °C, 0.5 slpm N_2 sweep gas, 2% Pt–1% Re/ $Ce_{0.5}Zr_{0.4}W_{0.1}O_2$.

The long gas production tail observed in the reactions may have been due to a number of factors, including reaction rates limited by the reforming or hydrolysis. To test whether the phenomena was due to a reforming limitation, such as catalyst deactivation or fouling, a used catalyst was reloaded and the reaction was repeated for cellulose without further processing of the catalyst. The resultant gas profiles were nearly identical, with conversion of 60%, indicating the tail was not due to catalyst deactivation. A high pressure liquid chromatography (HPLC) method was developed later and was used to confirm the formation of organic acid, such as formic and acetic acid in alkaline hydrolysis and reforming of woody biomass. These reactions are sensitive to temperature as well as base concentration, as described in Section 2.5.

When the experiments were repeated at 310 °C, the conversion increased with minimal loss of selectivity. Some loss of selectivity was observed for xylan due to an increased production of low molecular weight hydrocarbons, but this number was questionable due to an issue with the hydrocarbon gas analysis during the run. The reaction liquors were clear and colorless, as shown in Figure 42b and Figure 42d, a vast difference when compared to hydrolyzed-only samples (Figure 42a and Figure 42c). The white powdery material visible in the picture was determined to be a potassium titanate resulting from caustic attack on the titanium screen used to hold the catalyst. Potassium titanate formation is a known corrosion issue with titanium in alkaline environments at high temperatures.

2.4.2 Wood Component Study to Optimize Flow Reaction Conditions

After the demonstration of complete reforming of woody biomass to hydrogen in batch reactors, effort shifted to the development of a reactor system for continuous conversion of biomass to hydrogen. Use of a continuous stirred tank reactor (CSTR) was determined to be a promising approach. CSTR tests for cellulose were planned and carried out to examine the effect of residence time, base concentration/pH, and temperature on the H_2 yield and selectivity of the reforming. Figure 44 shows the set up of the reactor.

Figure 44: Continuous stirred tank reactor (CSTR) setup based on a 0.5 L Parr autoclave. Also shown is an insulated heat exchanger (recuperator) necessary to transfer heat from the CSTR effluent to the inlet for the autoclave heater to maintain a constant reaction temperature.

Initial experiments showed that cellulose reforming was not significant at 250 °C, consistent with the batch results above. At 275 °C, methane was the main reforming product, but there was very little gas produced. At 310 °C, H_2 became the main reforming product, though H_2 conversion was still low at a liquid residence time of 8 min. Therefore, more tests were carried out at 310 °C to examine the effect of liquid residence time and the amount of catalyst use in the CSTR. As shown in Figure 45, increasing the liquid feed residence time (τ_v) slightly increased the H_2 yield but had a negligible impact on the H_2 selectivity.

However, doubling the amount of catalyst from 60 g to 120 g had a larger impact, effectively doubling the H_2 yield but with a corresponding decrease in selectivity. Figure 46 shows this effect more clearly by plotting the yield and selectivity versus the catalyst to cellulose ratio (W/m) in the reactor. By doubling W/m from 7.5 to 15, the H_2 yield doubles with a slight increase in yield that can be attributed to increasing the liquid residence time.

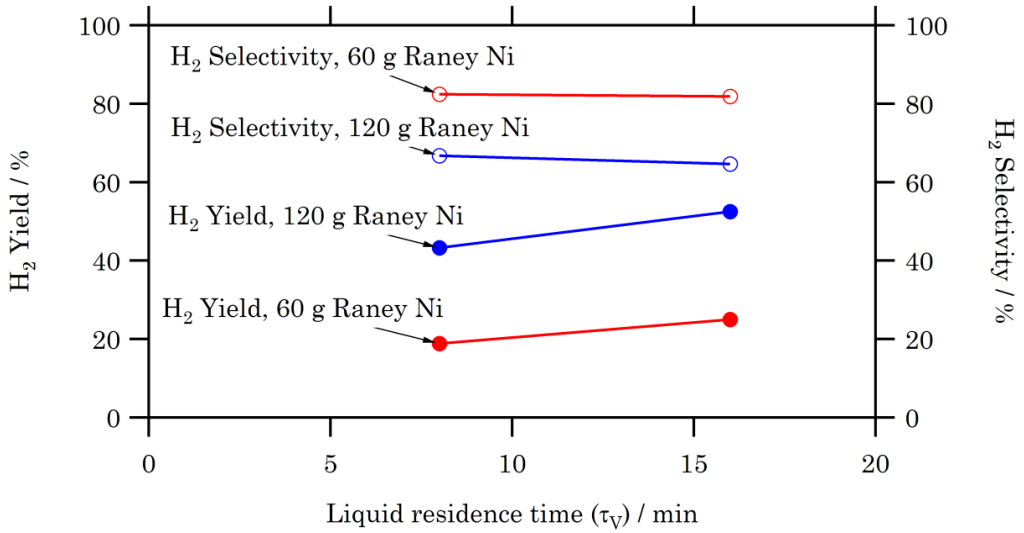

Figure 45: Effect of liquid residence time (reactor liquid volume/feed flow rate) on H_2 yield for cellulose reforming at 2% feed, 0.2 M K_2CO_3, 310 °C.

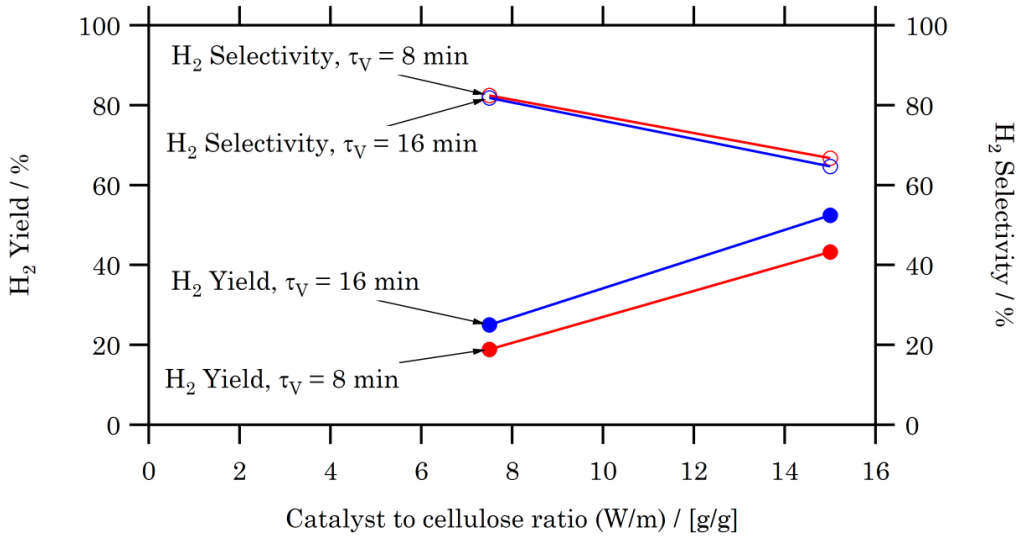

Figure 46: Effect of Raney Ni catalyst to cellulose ratio on H_2 yield for cellulose reforming at 2% feed, 0.2 M K_2CO_3, 310 °C.

The reaction of cellulose in the presence of base and a nickel catalyst can be considered to follow the reaction scheme shown below.

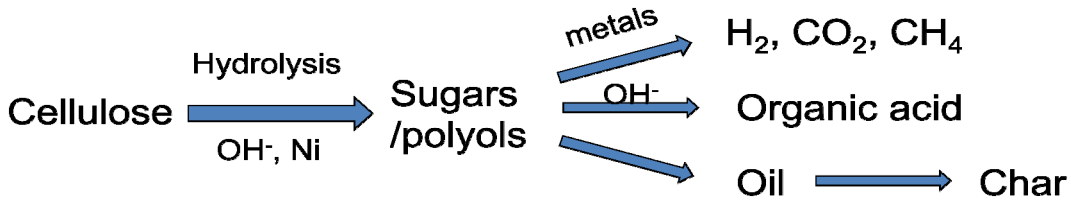

Hydrolysis of cellulose is catalyzed by both base and Ni catalyst, while the presence of base also inhibits the char formation, as shown in the literature [7]. The reforming of the resulting products, such as glucose, to gas is probably catalyzed by the Ni catalyst. The presence of base also catalyzes acid formation, as shown in both the literature [8] and UTRC modeling results for ethylene glycol reforming on Ni (Section 2.5).

Thus, with a fixed cellulose feed concentration, a fixed amount of Ni catalyst, and a fixed base concentration, the hydrolysis of cellulose is primarily determined by the liquid residence time, which is the ratio of the reactor volume to the total liquid feed rate. On the other hand, the relative amount of Raney Ni catalyst to the maximum total amount of cellulose in the CSTR reactor determines the extent of the reforming reaction.

The conversion results on cellulose in the CSTR indicated that cellulose hydrolysis is faster than reforming, and thus the H_2 yield was primary controlled by the reforming rate. By increasing the catalyst to cellulose ratio, reforming increased, resulting in improved H_2 yields. However, the H_2 yield was maximized around 55% over the range of conditions that were tested. This was probably due to the formation of organic acids. Krochta et al. have shown that a 40% yield of acid can be obtained from cellulose at 280 °C with 4% NaOH [8].

2.5 Atomistic and Thermodynamic Modeling

To understand the effect that the addition of base plays in the reforming process, thermodynamic modeling was performed at 300 °C considering the following reactions and their Gibbs free energies.

$$C_2H_6O_2 + 4KOH \longleftrightarrow 2K_2CO_3 + 5H_2 \quad \Delta G_{300°C} = -423\ \text{kJ/mol} \quad (1)$$

$$C_2H_6O_2 + 2KOH \longleftrightarrow K_2CO_3 + H_2O + CH_4 + H_2 \quad \Delta G_{300°C} = -315\ \text{kJ/mol} \quad (2)$$

$$C_2H_6O_2 + H_2O \longleftrightarrow H_2CO_3 + CH_4 + H_2 \quad \Delta G_{300°C} = -179\ \text{kJ/mol} \quad (3)$$

$$C_2H_6O_2 + 4H_2O \longleftrightarrow 2H_2CO_3 + 5H_2 \quad \Delta G_{300°C} = -111\ \text{kJ/mol} \quad (4)$$

The first two reactions show interactions with base and the last two with water. In the presence of base, formation of hydrogen gas is more energetically favorable, resulting in a high selectivity toward hydrogen. In pure aqueous reforming, reaction (3) is more exothermic than reaction (4) and both methane and hydrogen are present as reaction products.

First principles atomistic modeling was used to gain an insight into the factors that control the activity and selectivity toward hydrogen production by ethylene glycol reforming on Ni catalysts. The schematic diagram of reforming pathways is depicted in Figure 47. For ethylene glycol on a Ni surface, the first step after adsorption is hydroxyl bond breaking to form an ethylenedioxy intermediate. At the surface coverage considered, the activation of C-O bond in ethylenedioxy and rearrangement to form the acetaldehyde intermediate and adsorbed oxygen are thermodynamically favorable. Subsequent dehydrogenation and C-C

bond scission of acetaldehyde yields the CO and CH_3 as final decomposition intermediates. CO is shifted in water to CO_2 and H_2 while the methyl is hydrogenated into methane. In a basic environment, CO can also be converted to a formate ion in solution through hydrophilic attack, consistent with the experimental observation of formic acid in the spent liquor.

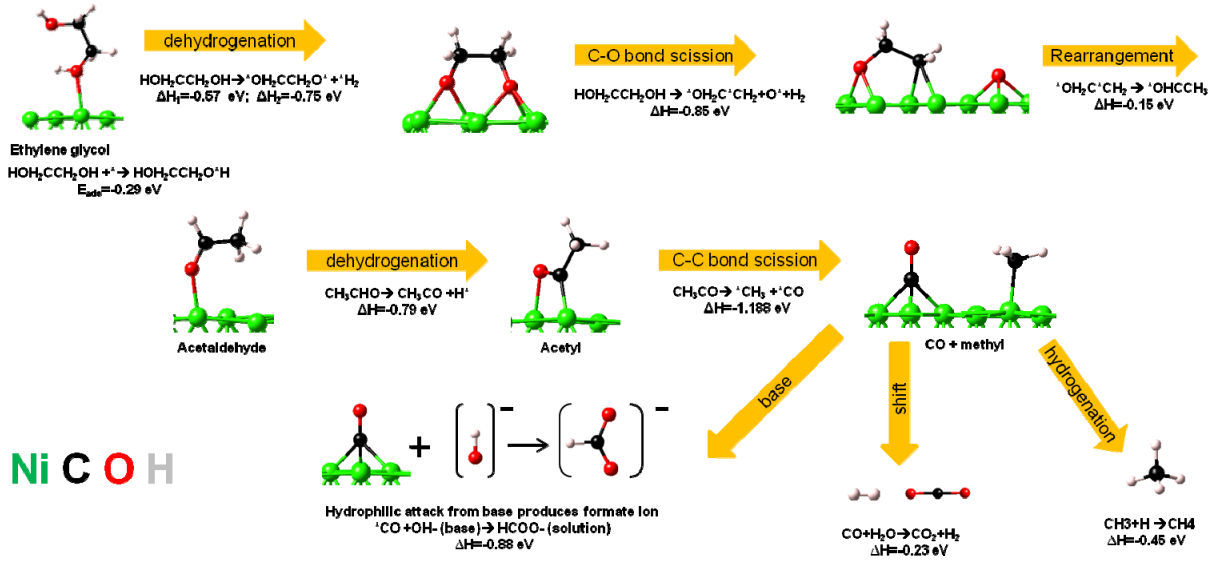

Figure 47: Atomistic modeling analysis of the reforming of ethylene glycol over Ni showing the intermediate reaction steps and the reaction enthalpies of their formation.

First principles atomistic modeling was also used to gain further insight into the factors that control the activity and selectivity toward hydrogen production by ethylene glycol reforming on Pt catalysts. Earlier testing work used Pt-based catalysts before switching to less expensive Ni-based catalysts, and it was worthwhile to understand the differences in reaction mechanisms.

A schematic diagram of the reforming pathways for ethylene glycol on Pt is depicted in Figure 48. For ethylene glycol on the Pt surface, the first steps after adsorption are dehydrogenations. Unlike Ni catalysts, Pt appears to prefer C-C breaking rather than C-O breaking as the first step. As a result, the dehydrogenated species does not go through an ethylenedioxy intermediate as is the case with Ni, but rather undergoes a direct C-C bond scission which results in two COH species.

The resulting COH groups can undergo a direct reaction with OH^- from the base to form CO_2 and H_2. Alternatively, the COH group can dehydrogenate further to a CO surface species which can react with hydrogen to form methane or be shifted in water to CO_2 and H_2 as happens with Ni. Also similar to the Ni case, the CO can be converted to a formate ion in solution through hydrophilic attack in a basic environment.

These modeling results offer an explanation as to why Pt-based catalysts favor reforming to H_2 while Ni prefers to form methane. **Ni-based catalysts prefer to break C-O bonds, which result in both the formation of a methyl group and a CO. Pt-based catalysts prefer to break C-C bonds, resulting in only CO species. The increased preference toward CO species most likely leads to an increase in hydrogen production over methane.**

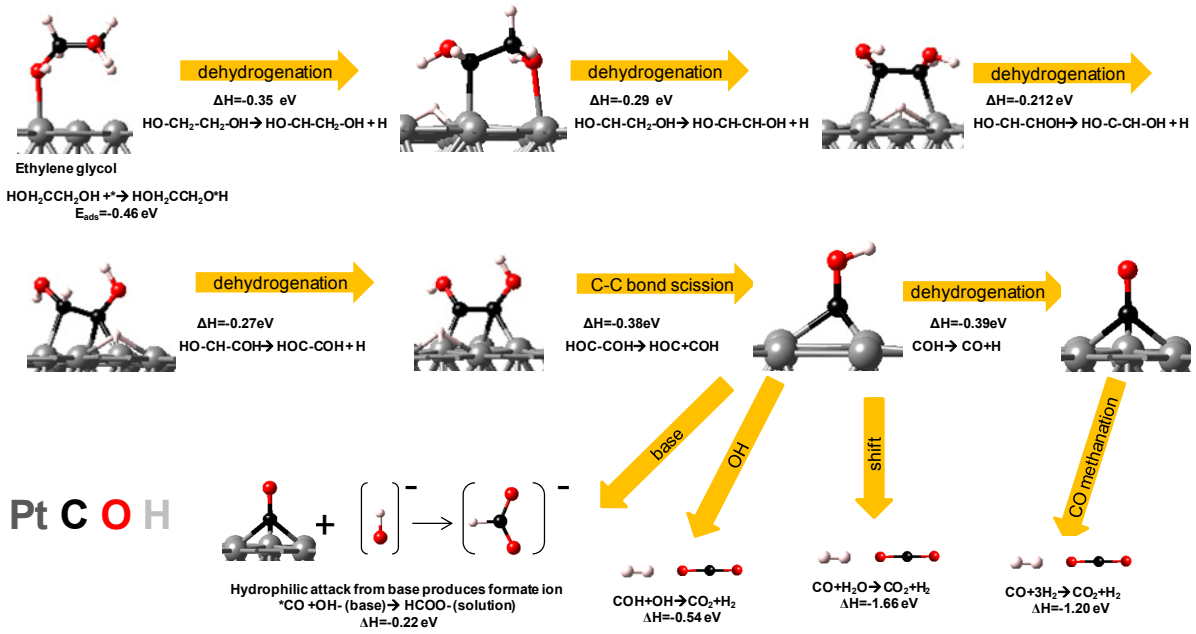

Figure 48: Atomistic modeling analysis of the reforming of ethylene glycol over Pt showing the intermediate reaction steps and the reaction enthalpies of their formation.

2.6 Demonstration System

Based on the successful work with base metal catalysts in the batch reactor with wood and the CSTR with cellulose, the final step of the project was the construction and testing of a demonstration unit for H_2 production. This continuous flow demonstration unit consisted of wood slurry and caustic feed pump systems, two reactors for hydrolysis and reforming, and a gas-liquid separation system. A schematic is shown in Figure 49. The technical challenges associated with unreacted wood fines and Raney Ni catalyst retention limited the demonstration unit to using a fixed bed Raney Ni catalyst. The lower activity of the larger particle Raney Ni in turn limited the residence time and thus the wood mass flow feed rate to 50 g min^{-1} for a 1 wt% wood slurry. The project demonstrated continuous flow H_2 yields with unmodified fixed bed Raney Ni of 63% to 100%, with corresponding H_2 selectivities of 6% to 21% for periods of several hours. The fixed bed form of the Raney Ni exhibited signs of deactivation which requires further study and may require further development of a more active and durable fixed-bed catalyst for the process.

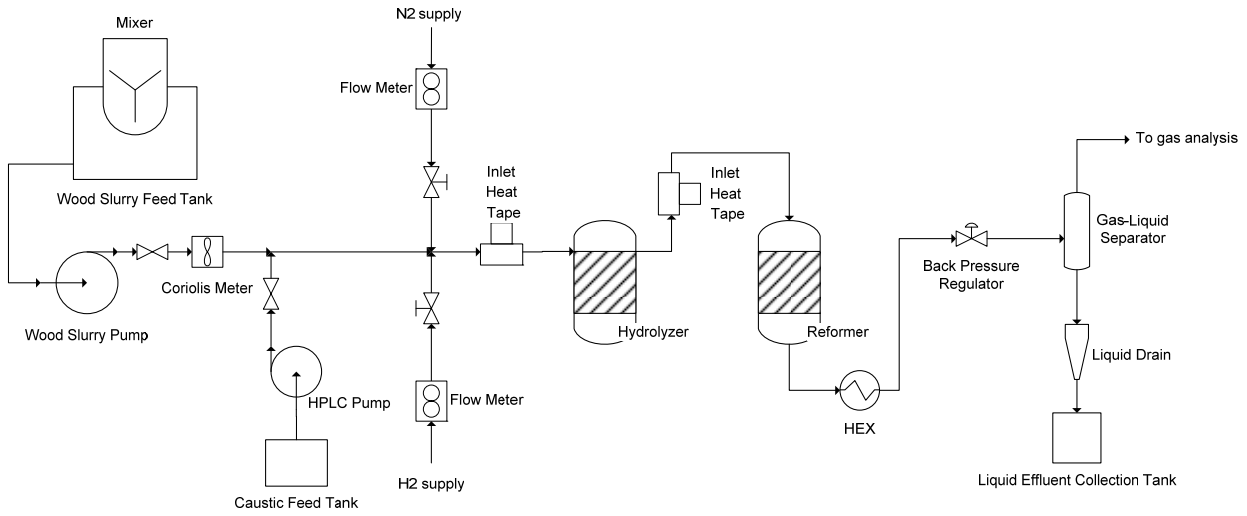

Figure 49: Schematic diagram of UTRC demonstration system.

Testing in the demonstrator system began with the model compound ethylene glycol for the purposes of validating the new set up. A key challenge for the flow reactor systems was catalyst retention. For more rapid development, it was decided to continue to use unpromoted nickel as the catalyst, recognizing that the initial results would have low H_2 selectivities (i.e., higher methane production). A simple catalyst based on loading nickel onto commercial, dense, rutile (titania) pellets was prepared based on UTRC's experience that the rutile pellets were resistant to the biomass reforming reaction conditions. The first test was done with a 2.5% ethylene glycol feed using nickel supported on rutile (TiO_2) as the reforming catalyst. As shown in Table 10, a H_2 yield of 77.4% and a H_2 selectivity of 76.3% were obtained with 50 g min^{-1} slurry feed rate. This was comparable to previous ethylene glycol testing results.

SEM characterization of the supported nickel pellets revealed that the catalyst pellets were missing nickel from the surface. Based on the changes in morphology on the exposed titania areas, the hot alkaline environment appeared to be affecting the surface of the pellets resulting in loss of nickel. Since the focus of the demonstration experimental effort was not on catalyst optimization, but rather process optimization and reactor geometry, no further attempts were made to improve the supported catalyst and the effort focused on Raney Ni.

Testing of the demonstrator system with a wood feed (1 wt%) proceeded under operating conditions similar to those used for the ethylene glycol run. Initially, an insignificant amount of H_2 was produced. Changes to the system setup, including the use of a powder Raney Ni catalyst and a sintered metal tube in the reactor exit to retain the Raney Ni, increased the H_2 yield to 29.8%, as shown in Table 10. The product liquor was a brownish suspension rather than a clear solution, as shown in Figure 50, indicating a significant amount of acid formation or insufficient break down of wood. The addition of H_2 during hydrolysis aids the break-down of the wood, especially the lignin component, to monocyclic species. Therefore, a small amount of H_2 (100 mL min^{-1}) was added to the reformer feed in an effort to increase H_2 yield.

The H_2 addition significantly increased the wood conversion, and a 78.9% H_2 yield (excluding the added H_2) was achieved compared to a 29.8% H_2 yield without the addition of H_2, as shown in Table 10. Figure 50 shows a picture of the product liquor from this

experiment, which was a clear solution, similar to what was obtained in the wood batch experiments described in Section 2.2.

Table 10: Test results from initial demonstrator set up using 1.8 L autoclave.

Feed	Slurry feed rate (g min^{-1})	Feed concentration (%)	K_2CO_3/Feed (g/g)	Reformer Temperature (°C)	H_2 yield (%)	H_2 selectivity (%)
Ethylene glycol	50	2.5	1.1	310	77.4	76.3
Wood flour (initial test)	49	1	1.04	310	2.1	56
Wood flour	56	1	0.9	310	29.8	83.8
Wood with 100 ml min^{-1} H_2 addition	41	1	1.34	310	78.6	36.1

Figure 50: Reaction product liquors from 1wt% wood runs with the proof-of-concept demonstration system at 310 °C. The brown liquor was produced with a slurry feed rate of 56 g min^{-1} with 0.9 K_2CO_3/wood. The clear, colorless liquor on the right resulted from a slurry feed rate of 4 g min^{-1} with 1.34 K_2CO_3/wood and the addition of 100 mL min^{-1} H_2 to the feed.

These initial runs provided the first successful demonstration of the conversion of wood to H_2 in a continuous flow reactor set up, but there was some difficulty in running tests longer than a few hours because of a buildup of pressure in the system. This pressure build up was caused by plugging of the sintered metal tube used to retain Raney Ni catalyst and unconverted wood particles inside the reactor, and within only a few hours it would progress to such a degree that the experiments had to be stopped. To avoid the plugging problems introduced by the sintered metal tube, the conventional powder Raney Ni was replaced by a fixed bed version of the Raney Ni catalyst. As long as the wood conversion was maintained at a high level, this system adjustment allowed the flow reactor to be operated for an entire day, including heat up and pressurization. However, low wood conversions could still result in carryover of unconverted wood particles, which eventually built up in downstream piping, forcing system shutdown because of system pressure rise.

Table 11 shows data obtained for four flow reactor experiments using the fixed bed version of the Raney Ni catalyst and a 1 wt% wood slurry. The fixed bed Raney Ni "chunks" had a lower surface area (≈10 m^2g^{-1}) and a lower packing density compared to the

conventional Raney Ni power (≈80 m^2g^{-1}). Each of the experiments was operated for 2 to 4 hours once the flow rate, temperatures, and pressures reached a steady state.

Table 11: Test results for Biomass to H_2 continuous flow system with 1% wood slurry and a fixed bed version of Raney Ni catalyst.

Feed	Slurry feed rate (g min^{-1})	Wood concentration (%)	K_2CO_3/Wood (g/g)	H_2 yield (%)	H_2 selectivity (%)	Carbon yield (%)
Wood flour	50.0	1	1.35	**103.8**	38.7	**81.1**
Wood flour	50.0	1	0	43.8	1.2	48.6
Wood flour	40.1	1	1.676	69.2	10.0	71.7
Wood flour	97.3	1	1.38	**25.2**	40.4	**44.0**

Figure 51 and Figure 52 show the hydrogen yield and selectivity, respectively, for the experiments given in Table 11 with a feed rate of approximately 50 g min^{-1}. The initial activity of the Raney Ni was good, with an average wood conversion based on carbon analysis of 81% and a hydrogen selectivity of 39%. A second experiment was performed with the same catalyst in which the base was not added to the feed and this resulted in a decrease in wood conversion to approximately 49% with a low hydrogen selectivity of approximately 1%. This was further evidence supporting the observation that the base increases the yield and selectivity of the process. When a third experiment was performed where the base was introduced into the feed, there was a reduced performance for the catalyst, with a conversion of only 72% and a selectivity of 10%, suggesting that the fixed bed Raney Ni catalyst was undergoing some form of deactivation.

To further explore the apparent deactivation of the fixed bed Raney Ni catalyst, a catalyst durability study was conducted in the demonstrator system. A fresh batch of fixed bed Raney Ni catalyst was loaded into the system and tested at a wood slurry flow rate of 50 g min^{-1}, wood concentration of 0.5 wt%, and a base concentration of 1.4 g K_2CO_3/g wood. The system was run for several hours, including an overnight shut down, to observe both the initial performance and the performance progression to steady state. The results of this testing are shown in Figure 53 and Figure 54. Initially the catalyst showed high wood conversion (average of 102% based on hydrogen) and hydrogen selectivity of 21%. However, both wood conversion and hydrogen selectivity decreased after about two hours of testing, reaching steady values of 63% and 6%, respectively. The overnight shutdown appeared to accelerate this performance degradation. This performance degradation was not observed for tests using Raney Ni in powder form. The reason for this apparent difference between the fixed bed and powder form of the Raney Ni catalyst could be the lower surface area (10 m^2g^{-1}) of the fix bed catalyst versus the powder (80 m^2g^{-1}), which could simply render deactivation more apparent in the fixed bed catalyst, but a definitive judgment on the root cause was not possible by the end of the project.

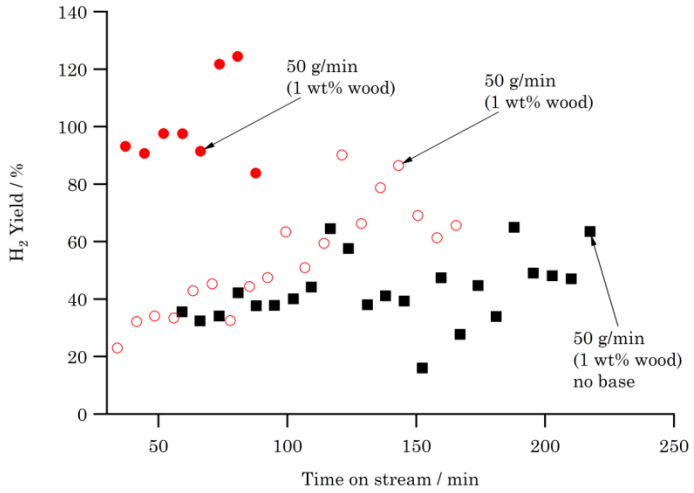

Figure 51: Hydrogen yield versus time for various flow reactor experiments using a 1 wt% wood slurry and a fixed bed Raney Ni catalyst.

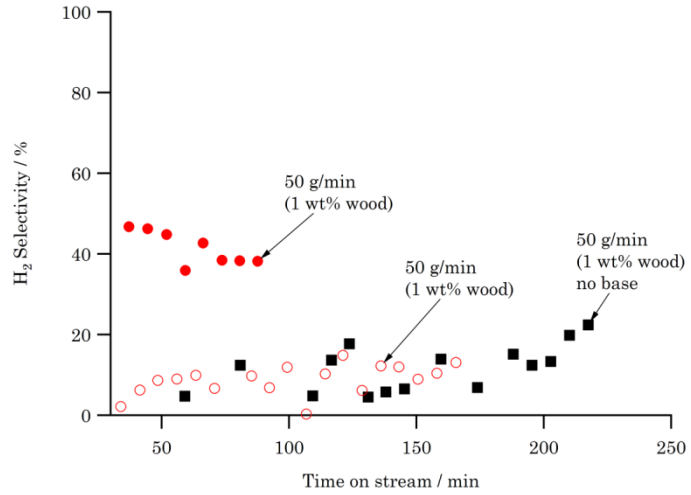

Figure 52: Selectivity to hydrogen versus time for various flow reactor experiments using a 1 wt% wood slurry and a fixed bed Raney Ni catalyst.

A common feature of all of the testing with wood in the demonstrator system using nickel catalysts was low selectivity to H_2 (see Table 11 and Figure 52). Previous results with Raney Ni powder in the batch autoclave indicated that the selectivity to H_2 of this catalyst can be improved by modifying the catalyst with dopants. A modification treatment was performed on the fixed bed Raney Ni, and this modified catalyst was tested in the flow system. The results of this testing are shown in Figure 53 and Figure 54. The average hydrogen selectivity of the modified Raney Ni catalyst was 25%, which was only slightly higher than the initial performance of the unmodified fixed bed Raney Ni (21%). This was in contrast to the selectivity increase that was previously observed for the modified powder Raney Ni, which showed an increase from ≈40% (unmodified) to ≈80% (modified) for ethylene glycol flow reactor tests with >85% yield. Again, the fixed bed version of the Raney Ni catalyst could be less selective, whether modified or unmodified, because its lower

surface area renders these performances more apparent than for the powder form of the catalyst, but a definitive judgment requires further study.

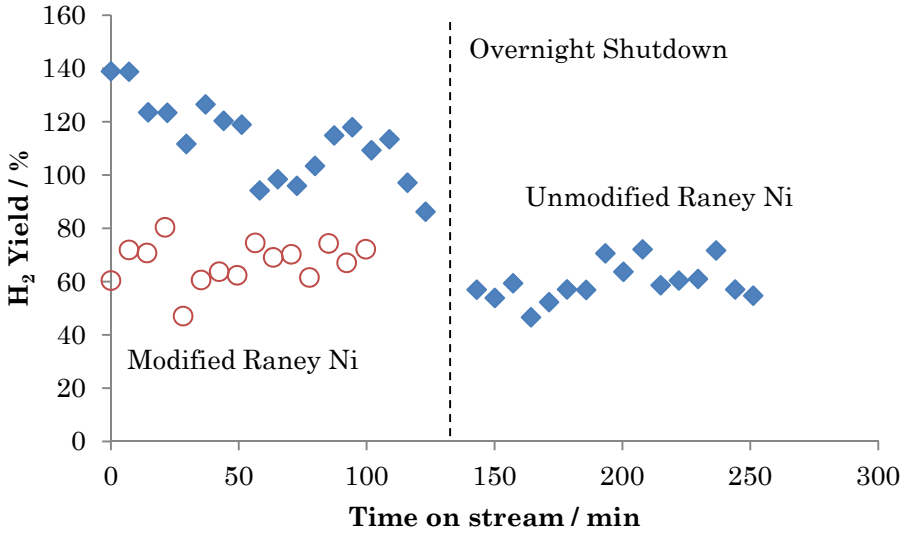

Figure 53: Hydrogen yield versus time for flow reactor experiments using 50 g min^{-1} of a 0.5 wt% wood slurry with a base concentration of 1.4 g K_2CO_3 / g wood and two different fixed bed Raney Ni catalysts. The modified Raney Ni catalyst data are indicated by open red circles.

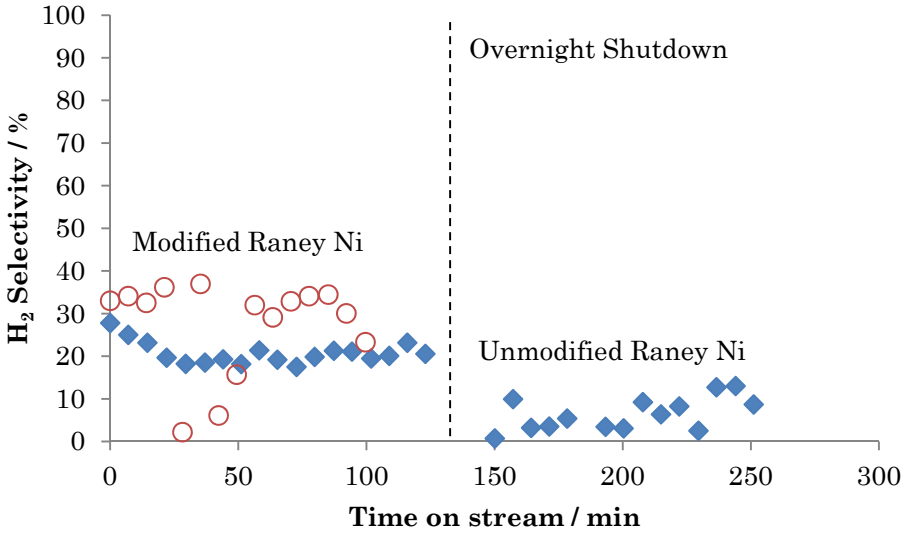

Figure 54: Selectivity versus time for flow reactor experiments using 50 g min^{-1} of a 0.5 wt% wood slurry with a base concentration of 1.4 g K_2CO_3 / g wood and two different fixed bed Raney Ni catalysts. The modified Raney Ni catalyst data are indicated by open red circles.

Testing in the demonstrator system with the fixed bed Raney Ni catalyst revealed that the activity and packing density of this catalyst was such that operation at slurry flow rates higher than 100 g min^{-1} and/or wood concentrations above 1 wt% resulted in conversions that were too low to allow for continuous operation of the system. At conditions exceeding these limits, unconverted wood solids plugged the system piping. To obtain data on the relationship between wood flow rate and conversion for the fixed bed Raney Ni (which is useful for reactor sizing), a series of tests were performed at a slurry flow rate of 54-66 g min^{-1} and wood concentrations between 0.25 wt% and 0.75 wt%. The catalyst used for this series of tests was the same material that had previously undergone the degradation study described above. That is, the catalyst had already reached its steady state performance. This data is summarized in Table 12.

Figure 55 shows this data plotted as hydrogen yield versus the ratio of catalyst to wood (g/g). As can be seen, there was no discernable trend in this data, indicating that the hydrogen yield was not strongly dependent on this parameter over this range of operating conditions. The lack of any trend in this data could be due to the narrow range of catalyst to wood ratio tested, which was limited by the wood concentrations and slurry flow rates accessible by the UTRC demonstration system. Table 12 also shows that tests were conducted both with and without hydrogen addition. These tests were conducted to determine the effect of a small amount of hydrogen addition on the system performance, which appeared to be minimal for this catalyst. This is in contrast to results obtained for Raney Ni in powder form, where hydrogen addition increased wood conversion, as described above and shown in Table 10.

Table 12: Test results for biomass to H_2 continuous flow system with fixed bed Raney Ni catalyst.

Wood Conc. (wt%)	H_2 Addition (mL min^{-1})	Feed Flow Rate (g min^{-1})	K_2CO_3/Feed (g/g)	Catalyst	H_2 Yield (%)	H_2 Selectivity (%)
0.50	100	62.1	1.3	Modified Fixed Bed Raney Ni	65.6	25.1
0.50	100	59.6	1.3	Fixed Bed Raney Ni (fresh)	102.1	21.0
0.50	100	64.8	1.3	Fixed Bed Raney Ni (from above)	62.7	6.4
0.50	0	63.1	1.3	Fixed Bed Raney Ni (from above)	59.1	38.1
0.25	0	59.6	1.3	Fixed Bed Raney Ni (from above)	67.2	42.2
0.375	0	65.6	1.3	Fixed Bed Raney Ni (from above)	42.5	36.3
0.50	0	53.6	1.3	Fixed Bed Raney Ni (from above)	79.7	34.8
0.75	0	54.6	1.3	Fixed Bed Raney Ni (from above)	52.8	29.6
0.25	0	58.5	1.3	Fixed Bed Raney Ni (from above)	82.4	40.6
0.375	0	60.6	1.3	Fixed Bed Raney Ni (from above)	61.9	34.2

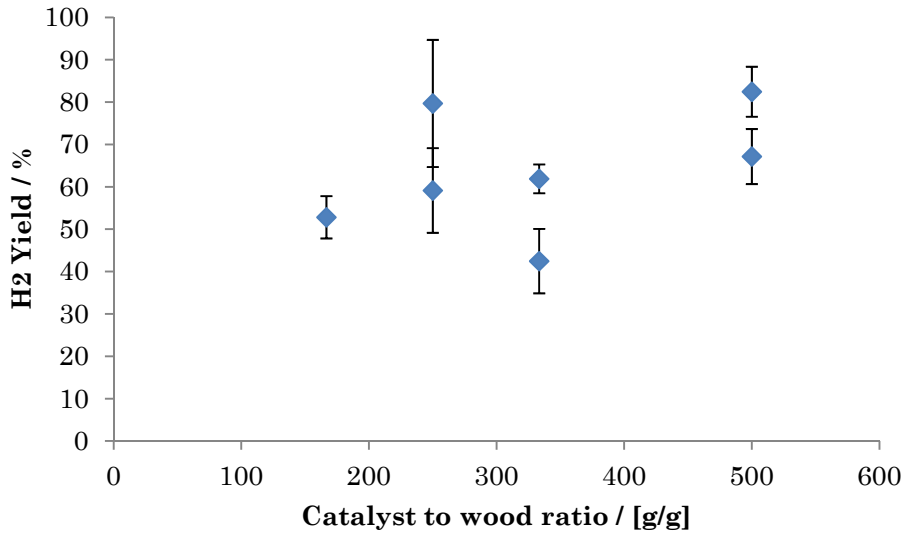

Figure 55: Hydrogen yield versus ratio of catalyst to wood for flow reactor experiments with fixed bed Raney Ni catalyst operating with no H_2 addition.

3 Conclusion

The project showed that it is possible to economically produce H_2 from woody biomass in a carbon neutral manner. Technoeconomic analyses using HYSYS and the DOE's H2A tool were used to design a 2000 ton day^{-1} (dry basis) biomass to hydrogen plant with an efficiency of 46% to 56%, depending on the mode of operation and economic assumptions, exceeding the DOE 2012 target of 43%. The cost of producing the hydrogen from such a plant would be in the range of \$1/kg H_2 to \$2/kg H_2.

The complete conversion of wood to hydrogen, methane, and carbon dioxide was repeatedly demonstrated in batch reactors varying in size from 50 mL to 7.6 L. The different wood sources (e.g., swamp maple, poplar, and commercial wood flour) were converted in the presence of a heterogeneous catalyst and base at relatively low temperatures (e.g., 310 °C) at sub-critical pressures sufficient to maintain the liquid phase.

Both precious metal and base metal catalysts were found to be active for the liquid phase hydrolysis and reforming of wood. Pt-based catalysts, particularly Pt-Re, were shown to be more selective toward breaking C-C bonds, resulting in a higher selectivity to hydrogen versus methane. Ni-based catalysts were found to prefer breaking C-O bonds, favoring the production of methane. The project showed that increasing the concentration of base (base to wood ratio) in the presence of Raney Ni catalysts resulted in greater selectivity toward hydrogen but at the expense of lower conversion of wood to gas due to increasing the production of undesirable organic acids from the wood. It was shown that by modifying Ni-based catalysts with dopants, it was possible to reduce the base concentration while maintaining the selectivity toward hydrogen and increasing wood conversion to gas versus organic acids.

The final stage of the project was the construction and testing of a demonstration unit for H_2 production. This continuous flow demonstration unit consisted of wood slurry and potassium carbonate feed pump systems, two reactors for hydrolysis and reforming, and a gas-liquid separation system. The technical challenges associated with unreacted wood fines and Raney Ni catalyst retention limited the demonstration unit to using a fixed bed

Raney Ni catalyst form. The lower activity of the larger particle Raney Ni in turn limited the residence time and thus the wood mass flow feed rate to 50 g min^{-1} for a 1 wt% wood slurry. The project demonstrated continuous flow H_2 yields with unmodified, fixed bed Raney Ni, from 63% to 100% with corresponding H_2 selectivities of 6% to 21%, for periods of several hours.

Additional development work is required before this process can be commercialized. There is potential in the nickel-based catalysts for an inexpensive process, but the durability and activity of these catalysts needs development. The catalyst kinetics, particularly in a flow reactor system, also require further development to enable better reactor sizing.

Once the laboratory-scale issues have been further investigated, additional effort should be placed on demonstrating the process on a larger scale. In particular, the research should move toward demonstrating >90% recycle of base and the development of a burner/reformer design for an integrated system. A larger scale demonstration should also be performed with power generation as its objective by coupling the process with a means to use the hydrogen, such as a fuel cell, gas turbine, or internal combustion engine.

4 Products & Technology Transfer Activities

Several presentations were given during the course of this project on the key modeling and experimental results. The results of the acid-based system modeling and optimization were presented at a 2006 ACS meeting [5]. In addition to the regular DOE Annual Merit Review presentations, the results for reforming of wood in a batch reactor completely to gas were presented at both the 21st North American Catalysis Society [9] and the 2010 AIChE Meeting [10].

This project used computing facilities at the Oak Ridge National Laboratory under DOE contract DE-AC05-00OR22725 to complement the resources at UTRC for atomistic modeling. In addition, a research license agreement was made with Virent Energy Systems in Madison, Wisconsin for the duration of this DOE project.

5 References

[1] Steward, D.M., *Hydrogen Analysis (H2A) Central Hydrogen Production Model Version 2.1*. 2008, U.S. Department of Energy NETL.

[2] *Hydrogen & Our Energy Future*. 2009, U.S. Department of Energy Hydrogen Program: Washington, DC.

[3] Curry-Nkansah, M.; Driscoll, D.; Farmer, R.; Garland, R.; Gruber, J.; Gupta, N.; Hershkowitz, F.; Holladay, J.; Nguyen, K.; Penev, M.; Schlasner, S.; Steward, D., *Hydrogen Production Roadmap: Technology Pathways to the Future*. 2009, U.S. Department of Energy: Energy Efficiency & Renewable Energy: Washington, DC.

[4] Rutkowski, M.; Kuehn, N.J., *Hydrogen Analysis (H2A) Central Hydrogen Production Model Version 1.0*. 2005, U.S. Department of Energy NETL.

[5] She, Y.; Emerson, S.C.; Vanderspurt, T.H., *Modeling and Simulation of Hydrogen Production from Biomass through Hydrolysis and Liquid-Phase Reforming Processes*, in *231st ACS Meeting*. 2006: Atlanta, GA.

[6] Kultikova, E.V., *Structure and Properties Relationships of Densified Wood*, in *Wood Science and Forest Products*. 1999, Virginia Polytechnic Institute and State University: Blacksburg, Virginia.

[7] Minowa, T.; Zhen, F.; Ogi, T., *Cellulose decomposition in hot-compressed water with alkali or nickel catalyst*. Journal of Supercritical Fluids, 1998. **13**: p. 253-259.

[8] Krochte, J.; Hudson, J.S.; Drake, C.W., *Alkaline thermochemical degradation of cellulose to organic acids.* Biotechnology and bioengineering symp., 1984(14): p. 37-54.

[9] Davis, T.D.; Emerson, S.C.; Campbell, T.A.; She, Y.; Willigan, R.R.; Vanderspurt, T.H., *Aqueous Phase Reforming of Yellow Poplar to Hydrogen*, in *21st North American Catalysis Society Meeting*. 2009: San Francisco, CA.

[10] Davis, T.D.; Emerson, S.C.; Zhu, T.; Willigan, R.R.; Peles, A.; She, Y.; Vanderspurt, T.H., *Liquid Phase Reforming of Wood Flour to Hydrogen*, in *2010 AIChE Annual Meeting*. 2010: Salt Lake City, UT.